Leveraging 35 years of *Pinus taeda* research in the southeastern U.S. to constrain forest carbon cycle predictions: regional data assimilation using ecosystem experiments

R. Quinn Thomas[1*], Evan B. Brooks[1], Annika L. Jersild[1], Eric J. Ward[2], Randolph H. Wynne[1], Timothy J. Albaugh[1], Heather Dinon Aldridge[3], Harold E. Burkhart[1], Jean-Christophe Domec[4,5], Thomas R. Fox[1], Carlos A. Gonzalez-Benecke[6], Timothy A. Martin[7], Asko Noormets[8], David A. Sampson[9], Robert O. Teskey[10]

[1]Department of Forest Resources and Environmental Conservation, Virginia Tech, USA
[2]Climate Change Science Institute and Environmental Sciences Division, Oak Ridge National Laboratory, USA
[3]State Climate Office of North Carolina, North Carolina State University, USA
[4]Bordeaux Sciences Agro, UMR 1391 INRA-ISPA, Gradignan Cedex, France
[5]Nicholas School of the Environment, Duke University, USA
[6]Department of Forest Engineering, Resources and Management, Oregon State University, USA
[7]School of Forest Resources and Conservation, University of Florida, USA
[8]Department of Forestry and Environmental Resources, North Carolina State University, USA
[9]Decision Center for a Desert City, Arizona State University, USA
[10]Warnell School of Forestry and Natural Resources, University of Georgia, USA

*Corresponding author: R. Quinn Thomas (rqthomas@vt.edu)

Abstract

Predicting how forest carbon cycling will change in response to climate change and management depends on the collective knowledge from measurements across environmental gradients, ecosystem manipulations of global change factors, and mathematical models. Formally integrating these sources of knowledge through data assimilation, or model-data fusion, allows the use of past observations to constrain model parameters and estimate prediction uncertainty. Data assimilation (DA) focused on the regional scale has the opportunity to integrate data from both environmental gradients and experimental studies to constrain model parameters. Here, we introduce a hierarchical Bayesian DA approach (Data Assimilation to Predict Productivity for Ecosystems and Regions, DAPPER) that uses observations of carbon stocks, carbon fluxes, water fluxes, and vegetation dynamics from loblolly pine plantation ecosystems across the Southeastern U.S. to constrain parameters in a modified version of the 3-PG forest growth model. The observations included major experiments that manipulated atmospheric carbon dioxide (CO_2) concentration, water, and nutrients, along with non-experimental surveys that spanned environmental gradients across an 8.6×10^5 km^2 region. We optimized regionally representative posterior distributions for model parameters, which dependably predicted data from plots withheld from the data assimilation. While the mean bias in predictions of N fertilization experiments, irrigation experiments, and CO_2 enrichment experiments was low, future work needs to focus modifications to model structure that decrease the bias in predictions of drought experiments. Predictions of how growth responded to elevated CO_2 strongly depended on whether ecosystem experiments were assimilated and whether the assimilated field plots in the CO_2 study were allowed to have different mortality parameters than the other field plots in the region. We present predictions of stem biomass productivity under elevated CO_2,

decreased precipitation, and increased nutrient availability that include estimates of uncertainty for the Southeastern U.S. Overall, we: 1) demonstrated how three decades of research in southeastern U.S. planted pine forests can be used to develop DA techniques that use multiple locations, multiple data streams, and multiple ecosystem experiment types to optimize parameters, and 2) developed a tool for the development of future predictions of forest productivity for natural resource managers that leverage a rich dataset of integrated ecosystem observations across a region.

1 Introduction

Forest ecosystems absorb and store a large fraction of anthropogenic carbon dioxide (CO_2) emissions (Le Quere et al., 2015; Pan et al., 2011) and supply wood products to a growing human population (Shvidenko et al., 2005). Therefore, predicting future carbon sequestration and timber supply is critical for adapting forest management practices to future environmental conditions and for using forests to assist with the reduction of atmospheric CO_2 concentrations. The key sources of information for developing these predictions are results from global change ecosystem manipulation experiments, observations of forest dynamics across environmental gradients, and process-based ecosystem models. The challenge is integrating these three sources into a common framework for creating probabilistic predictions that provide information on both the expected future state of the forest and the probability distribution of those future states.

Data assimilation (DA), or data-model fusion, is an increasingly used framework for integrating ecosystem observations into ecosystem models (Luo et al., 2011; Niu et al., 2014; Williams et al., 2005). DA integrates observations with ecosystem models through statistical, often Bayesian, methods that can generate probability distributions for ecosystem model parameters and initial states. DA allows for the explicit accounting of observational uncertainty (Keenan et al., 2011), the incorporation of multiple types of observations with different time scales of collection (MacBean et al., 2016; Richardson et al., 2010), and the representation of prior knowledge through informed parameter prior distributions or specific relationships among parameters (Bloom and Williams, 2015).

Using DA to parameterize ecosystem models with observations from multiple locations that

89 leverage ecosystem manipulation experiments and environmental gradients will allow for
90 predictions to be consistent with the rich history of global change research in forest ecosystems.
91 Ecosystem manipulation experiments provide a controlled environment in which data collected
92 can be used to describe how forests acclimate and operate under altered environmental
93 conditions (Medlyn et al., 2015) and can potentially allow for the optimization of model
94 parameters associated with the altered environmental factor in the experiment. Furthermore, the
95 assimilation of data from ecosystem manipulation experiments may increase parameter
96 identifiability (reducing equifinality; Luo et al., 2009), where two parameters have compensating
97 controls on the same processes, by isolating the response to a manipulated driver. Observations
98 that span environmental gradients include measures of forests ecosystem stocks and fluxes across
99 a range of climatic conditions, nutrient availabilities, and soil water dynamics. These studies
100 leverage time and space to quantify the sensitivity of forest dynamics to environmental variation.
101 However, covariation of environmental variation can pose challenges separating the responses to
102 individual environmental factors. Overall, assimilating observations from a region that includes
103 environmental gradients and manipulation experiments is a useful extension of prior DA research
104 focused on DA at a single site with multiple types of observations (Keenan et al., 2012;
105 Richardson et al., 2010; Weng and Luo, 2011).
106
107 Southeastern U.S. planted pine forests are ideal ecosystems for exploring the application of DA
108 to carbon cycle and forest production predictions. These ecosystems are dominated by loblolly
109 pine (*Pinus taeda* L.), thus allowing for a single parameter set to be applicable to a large region
110 containing many soil types and climatic gradients. Loblolly pine represents more than one half of
111 the standing pine volume in the southern United States (11.7 million ha) and is by far the single

most commercially important forest tree species for the region, with more than 1 billion seedlings planted annually (Fox et al., 2007; McKeand et al., 2003). There is also a rich history of experimental research located across the region focused on global change factors that have included nutrient addition (Albaugh et al., 2016; Carlson et al., 2014; Raymond et al., 2016), water exclusion (Bartkowiak et al., 2015; Tang et al., 2004; Ward et al., 2015; Will et al., 2015), and water addition experiments (Albaugh et al., 2004; Allen et al., 2005; Samuelson et al., 2008). The region also includes a multi-year ecosystem CO_2 enrichment study (McCarthy et al., 2010). Furthermore, many of these experiments are multi-factor with water exclusion by nutrient addition (Will et al., 2015), water addition by nutrient addition (Albaugh et al., 2004; Allen et al., 2005; Samuelson et al., 2008), and CO_2 by nutrients addition treatments (McCarthy et al., 2010; Oren et al., 2001). Beyond experimental treatments, Southeastern U.S. loblolly pine ecosystems include at least two eddy-covariance sites with high frequency measurements of C and water fluxes along with biometric observations over many years (Noormets et al., 2010; Novick et al., 2015), and sites with multi-year sap flow data (Ewers et al., 2001; Gonzalez-Benecke and Martin, 2010; Phillips and Oren, 2001). Finally, there are studies that include plots that span the regional environmental gradients and extend back to the 1980s (Burkhart et al., 1985). Overall, the multi-decadal availability of observations of C stocks (or biomass), leaf area index (LAI), C fluxes, water fluxes, and vegetation dynamics in plots with experimental manipulation and plots across environmental gradients, is well suited to potentially constrain model parameters and predictions of how carbon cycling responds to environmental change.

Using loblolly pine plantations across the southeastern U.S as a focal application, our objectives were to 1) develop and evaluate a new DA approach that integrates diverse data from multiple

locations and experimental treatments with an ecosystem model to estimate the probability distribution of model parameters, 2) examine how the predictive capacity and optimized parameters differ between an assimilation approach that only uses environmental gradients and an assimilation approach that uses both environmental gradients and ecosystem manipulations, and 3) demonstrate the capacity of the DA approach to predict, with uncertainty, regional forest dynamics by simulating how forest productivity responds to drought, nutrient fertilization, and elevated atmospheric CO_2 across the Southeastern U.S.

2 Methods

2.1 Observations

We used thirteen different data streams from 294 plots at 187 unique locations spread across the native range of loblolly pine trees to constrain model parameters (Table 1; Figure 1). The data streams covered the period between 1981 to 2015. The Forest Modeling Research Cooperative (FMRC) Thinning Study provides the largest number of plots that span the region (Burkhart et al., 1985). In this study, we only used the control plots that were not thinned. The Forest Productivity Cooperative (FPC) Region-wide 18 (RW18) study included control and nutrient fertilization addition plots that span the region (134.4 kg ha^{-1} N + 13.44 kg ha^{-1} P biannually) (Albaugh et al., 2015). The PINEMAP study included four locations dispersed across the region that included a replicated factorial experiment with control, nutrient fertilization (224 kg ha^{-1} N + 27 kg ha^{-1} P + micronutrients once at project initiation), throughfall reduction (30% reduction), and fertilization by throughfall treatments (Will et al., 2015). The SETRES study was located at a single location and included replicated control, irrigation (~650 mm of added water per year),

158 nutrient fertilization (~100 kg N ha^{-1} + 17 kg P ha^{-1} with micronutrients applied annually with
159 absolute amount depending on foliar nutrient ratios), and fertilization by irrigation treatments
160 (Albaugh et al., 2004). The Waycross study was a single site with a non-replicated fertilization
161 treatment. The annual application of nutrient fertilization was focused on satisfying the nutrient
162 demand by the trees and resulted in one most productive stands in the region (Bryars et al.,
163 2013). These five studies included data streams of stand stem biomass (defined as the sum of
164 stemwood, stembark and branches) and live stem density. Waycross and SETRES included LAI
165 measurements from litterfall traps (Waycross) or estimates from LICOR LAI-2200 (SETRES).
166 SETRES also included fine root and coarse root measurements. In the PINEMAP, SETRES, and
167 RW18 studies we only used foliage biomass estimates from the control plots. We excluded the
168 foliage biomass estimates from the treatment plots because they were derived from allometric
169 models that may not have captured changes in allometry due to the experimental treatment. We
170 did use LAI measurements from both control and treatment plots where available (SETRES).
171
172 We also included observations the Duke FACE study where the atmospheric CO_2 was increased
173 by 200 ppm above ambient concentrations. Based on the data presented in McCarthy et al.
174 (2010) the study included six control plots, four CO_2 fumigated rings (including the unfertilized
175 half of the prototype), two nitrogen fertilization treatments (115 kg N ha^{-1} yr^{-1} applied annually) ,
176 and one CO_2 by nitrogen addition treatment (fertilized half of prototype). The Duke FACE study
177 included observations of stem biomass (loblolly pine and hardwood), coarse root biomass
178 (loblolly pine and hardwood), fine root biomass (combined loblolly pine and hardwood), stem
179 density (loblolly pine only), leaf turnover (combined loblolly pine and hardwood), fine root
180 production (combined loblolly pine and hardwood), and monthly LAI (loblolly pine and

hardwood).

Finally, we included two Ameriflux sites with eddy-covariance towers in loblolly pine stands. The US-DK3 site was located in the same forest as the Duke FACE site described above (Novick et al., 2015). The US-NC2 site was located in coastal North Carolina (Noormets et al., 2010). We used monthly gross ecosystem production (GEP; modeled gross primary productivity from net ecosystem exchange measured at an eddy-covariance tower) and evapotranspiration (ET) estimates from the sites. The monthly GET and ET were gap-filled by the site PI. The GEP was a flux partitioned product created by the site PI. The biometric data from the US-DK3 site was assumed to be the same as the first control ring. The biometric data from the US-NC2 site included observations of stem biomass (loblolly pine and hardwood), coarse root biomass (loblolly pine and hardwood), fine root biomass (combined loblolly pine and hardwood), stem density (loblolly pine only), leaf turnover (combined loblolly pine and hardwood), and fine root production (combined loblolly pine and hardwood).

2.2 Ecosystem Model

We used a modified version of the Physiological Principles Predicting Growth (3-PG) model to simulate vegetation dynamics in loblolly pine stands (Bryars et al., 2013; Gonzalez-Benecke et al., 2016; Landsberg and Waring, 1997). 3-PG is a stand-level vegetation model that runs at the monthly time-step and includes vegetation carbon dynamics and a simple soil water bucket model (Figure 2). While a complete description of the 3-PG model and our modifications can be found in the Supplemental Material Section 1, the key concept for interpreting the results is that gross primary productivity (GPP) was simulated using a light-use efficiency approach where the

absorbed photosynthetically active radiation (APAR) was converted to carbon based on a quantum yield (Supplemental Material Section 1.1). Quantum yield was simulated using a parameterized maximum quantum yield (alpha) that was modified by environmental conditions including atmospheric CO_2, available soil water (ASW) and soil fertility (Supplemental Material Section 1.2-1.3). The ASW and soil fertility modifiers were values between 0 and 1, while the atmospheric CO_2 modifier had a value of 1 at 350 ppm (thus values greater than 1 at higher CO_2 concentrations).

Elevated CO_2 modified tree physiology by increasing quantum yield, based on an increasing but saturating relationship with atmospheric CO_2 (Supplemental Material Section 1.2). Based on initial results from the data assimilation, we also added a function where the allocation to foliage relative to stem biomass decreased as atmospheric CO_2 increased (Supplemental Material Section 1.2). ASW and quantum yield were positively related through a logistic relationship between relative ASW and the quantum yield modifier, where relative ASW was the ratio of simulated ASW to a plot-level maximum ASW. Soil fertility and quantum yield were proportionally related, where quantum yield was scaled by an estimate of relative stand-level fertility (a value of 1 was the maximum fertility). The fertility modifier (FR) was constant throughout a simulation of a plot and was either based on site characteristics or directly optimized as a stand-level parameter (Supplemental Material Section 1.3). For plots with nutrient fertilization, FR was a directly optimized parameter or set to 1, depending on the level of fertilization (see below). For unfertilized plots, we used site index (SI), a measure of the height of a stand at a specified age (25 years), to estimate FR. This approach is in keeping with previous efforts (Gonzalez-Benecke et al., 2016; Subedi et al., 2015); however, SI does not solely represent nutrient availability of an

ecosystem. For a given climate SI captures differences in soil fertility, where a lower SI corresponded to a site with lower fertility, but regional variation in SI also included the influence of climate on growth rates that were already accounted for in the other environmental modifiers in the 3-PG model. When a climate term is not used in the empirical FR model, FR is relative to the highest SI in the region, which does not occur in the northern extent of the region even in fertilized plots due to climatic constraints. Thus, we also included the historical (1970-2011) 35-year mean annual temperature (MAT) as an additional predictor, resulting in an empirical relationship that predicted FR as an increasing, but saturating, function of SI within areas of similar long-term temperature. For our application of the 3-PG model using DA, we removed the previously simulated dependence of total root allocation on FR (Bryars et al., 2013; Gonzalez-Benecke et al., 2016) because we separated coarse and fine roots. Other environmental conditions influenced GPP, including temperature, frost days, and vapor pressure deficit (VPD). A description of these modifiers can be found in Supplemental Material Section 1.2.

Each month, net primary production (a parameterized and constant proportion of GPP) was allocated to foliage, stem (stemwood, stembark, and branches), coarse roots, and fine roots (Supplemental Material Section 1.4). Differing from previous applications of 3-PG to loblolly pine ecosystems, we modified the model to simulate fine roots and coarse roots separately. 3-PG also simulated simple population dynamics by including stem density as a state variable. Stem density and stem biomass pools were reduced by both density-dependent mortality, based on the concept of self-thinning (Landsberg and Waring, 1997), and density-independent mortality, a new modification where a constant proportion of individuals die each month (Supplemental Material Section 1.5). Finally, we added a simple model of hardwood understory vegetation to

enable the assimilation GEP and ET observations from eddy-covariance tower studies with significant understories (Supplemental Material Section 1.7).

The water cycle was a simple bucket model with transpiration predicted using a Penman-Monteith approach (Bryars et al., 2013; Gonzalez-Benecke et al., 2016; Landsberg and Waring, 1997)(Supplemental Material Section 1.6). The canopy conductance used in the Penman-Monteith subroutine was modified by environmental conditions. The modifiers included the same ASW and VPD modifier as used in the GPP calculation. Maximum canopy conductance occurred when simulated LAI exceeded a parameterized value of LAI (LAIgcx). Evaporation was equal to the precipitation intercepted by the canopy. Runoff occurred when the ASW exceeded a plot-specific maximum ASW. As in prior applications of 3-PG, ASW was not allowed take a value below a minimum ASW, resulting in an implicit irrigation in very dry conditions. This assumption may cause the model to be less sensitive to low ASW but the optimized parameterization may compensate.

The 3-PG model used in this study simulated the monthly change in eleven state variables per plot: four stocks for loblolly pines, five stocks for understory hardwoods, loblolly pine stem density (stems ha^{-1}), and ASW. The key fluxes that were used for DA included monthly GEP, monthly ET, annual root turnover, and annual foliage turnover. In total, 46 parameters were required by 3-PG. The model required mean daily maximum temperature, mean daily minimum temperature, mean daily PAR, total frost days per month, total rain per month, annual atmospheric CO_2, and latitude. Each plot also required maximum ASW, SI, MAT, and the initial condition of the eleven state variables as model inputs (Figure 3).

We used the first observation at the plot as the initial conditions for the loblolly pine vegetation states (foliage biomass, stem biomass, coarse root biomass, fine root biomass, and stem number). When observations of coarse biomass and fine root biomass were not available, these stocks were initialized as a mean region-wide proportion of the observed stem biomass. However, the value of initial root biomass in plots without observations was not important because root biomass did not influence any other functions in the model. The hardwood understory stocks at US-DK3 and US-NC2 were also initialized using the first set of observations. Initial fine root and coarse biomass were distributed between loblolly pine and hardwoods based on their relative contribution of total initial foliage biomass. The initialized ASW was assumed to be equal to the maximum ASW because most plots were initialized in winter months when plant demand for water was minimal. The maximum ASW in each plot was extracted from the SSURGO soils dataset (Soil Survey Staff, 2013). The value we used corresponded to the maximum ASW for the top 1.5 m of the soil. We assumed that the minimum ASW was zero. Because we focused on a region-wide optimization, we used region-wide 4-km estimates of observed monthly meteorology as inputs and to calculate the 35-year MAT for each plot (Abatzoglou, 2013). SI was based on height measurements at age 25 in each plot or calculated by combining observations of height at younger ages with an empirical model (Dieguez-Aranda et al., 2006).

We simulated ecosystem manipulation experiments in the 3-PG model by altering the environmental modifiers or by modifying the environmental inputs. Nutrient addition experiments were simulated by setting FR equal to 1 for the studies that applied nutrients at regular interval to remove nutrient deficiencies (RW18, SETRES, Waycross). FR was directly

296 estimated for fertilized plots in two of the studies either because nutrients were only added once
297 at the beginning of the study (PINEMAP), thus potentially not removing nutrient limitation, or
298 nitrogen was the only element added (Duke FACE), thus allowing the potential for nutrient
299 limitation by other elements. For these plots, we also assumed that the FR of the fertilized plot
300 was equal to or larger than the control plot. Throughfall exclusion experiments were simulated
301 by decreasing the throughfall by 30% in the treatment plots. The SETRES irrigation experiments
302 were simulated by adding 650 mm to ASW between April and October. CO_2 enrichment
303 experiments were simulated by setting the atmospheric CO_2 input equal to the treatment mean
304 from the elevated CO_2 rings (570 ppm). One plot (US-NC2) included a thinning treatment during
305 the period of observation. We simulated the thinning by specifying a decrease in the stem count
306 that matched the proportion removed at the site, with the biomass of each tree equivalent to the
307 average of trees in the plot.
308
309 **2.3 Data assimilation method**
310 We used a hierarchal Bayesian framework to estimate the posterior distributions of parameters,
311 latent states of stocks and fluxes, and process uncertainty parameters. The latent states
312 represented a value of the stock or flux before uncertainty was added through measurement. The
313 approach was as follows.
314
315 Consider a stock or flux (m) for a single plot (p) at time t ($q_{p,m,t}$). $q_{p,m,t}$ is influenced by the
316 processes represented in the 3-PG model and a normally distributed model process error term,
317
318 $$q_{p,m,t} \sim \mathrm{N}(\mathrm{f}(\boldsymbol{\theta}, \mathrm{FR_p}), \sigma_m) \qquad \text{Equation 1}$$

where $\boldsymbol{\theta}$ is a vector of parameters that are optimized, FR_p is the site fertility, and σ_m is the model process error. Not shown are the vector of parameters that were not optimized (Supplemental Material Table 1), the plot ASW, an array climate inputs, and the initial conditions because these were assumed known and not estimated in the hierarchical model. The process error assumed that the error linearly scales with the magnitude of the prediction:

$$\sigma_m^2 = \gamma_m + \rho_m \mathrm{f}(\boldsymbol{\theta}, \mathrm{FR_p}) \qquad \text{Equation 2}$$

While the structure of the Bayesian model allowed for all data streams to have process uncertainty that scales with the prediction, in this application we only allowed stem biomass, GEP, and ET process uncertainty to scale because they had large variation across space (stem biomass) and through time (i.e., there should be lower process uncertainty in the winter when GEP is lower). For the other data streams, the linear scaling term was removed by fixing ρ_m at 0.

FR_p did not have an explicit probability distribution. Rather the probability density evaluated to 1 if the plot was not fertilized, thus causing FR_p to be estimated from SI and MAT (Supplemental Material Equation 15), or if it was a fertilized plot and has an FR_p equal or higher than that of its non-fertilized control plot. The probability density evaluated to 0 if the estimated FR_p in a fertilized plot was less than the FR_p in the control plot or FR_p was not contained in the interval between 0 and 1.

341 $$FR_p \sim \begin{cases} 1 \text{ if non-fertilized, } FR_p \geq 0, \text{ and } FR_p \leq 1 \\ 1 \text{ if } FR_p = 1 \text{ and fertilization levels are assumed to remove nutrient deficiencies} \\ 0 \text{ if } FR_p < 1 \text{ and fertilization levels are assumed to remove nutrient deficiencies} \\ 1 \text{ if fertilized but levels are not assumed to remove deficiencies and } FR_p \geq FR \text{ of control plot} \\ 0 \text{ if fertilized but levels are not assumed to remove deficiencies and } FR_p < FR \text{ of control plot} \\ 0 \text{ if } FR_p < 0 \text{ or } FR_p > 1 \end{cases}$$

342 Equation 3

343

344 Our model included the effect of observational errors for measurements of stocks and fluxes.
345 For a single stocks or flux for a plot at time t there was an observation ($y_{p,m,t}$). The normally
346 distributed observation error model was:

347

348 $$y_{p,m,t} \sim N(q_{p,m,t}, \tau^2_{p,m,t})$$ Equation 4

349

350 where $\tau^2_{p,m,t}$ represented the measurement error of the observed state or flux. By including the
351 observational error model, $q_{p,m,t}$ represented the latent, or unobserved, stock or flux. The variance
352 was unique to each observation because it was represented as a proportion of the observed value.
353 The $\tau^2_{p,m,t}$ was assumed known (Table 1) and not estimated in the hierarchical model.

354

355 The hierarchical model required prior distributions for all optimized parameters, including the
356 parameters for the 3-PG model (θ), FR_p, and the process error parameters. The prior
357 distributions for $\boldsymbol{\theta}$ are specified in Table 3. Some parameters were informed by previous
358 research in loblolly pine ecosystems while other parameters were 'uninformative' with flat
359 distributions that with broad, but physically reasonable, bounds. The prior distributions for the
360 process error parameters were non-informative and had a uniform distribution with upper and

lower bounds that spanned the range of reasonable error terms.

$$\gamma_m \sim U(0.001,100) \quad \text{Equation 5}$$

$$\rho_m \sim U(0,10) \quad \text{Equation 6}$$

By combining the data, process, and prior models, our joint posterior that includes all thirteen data streams, plots, months with observations, and fitted parameters was

$$p(\boldsymbol{\theta}, \boldsymbol{\gamma}, \boldsymbol{\rho}, \boldsymbol{q} | \boldsymbol{y}, \boldsymbol{\tau}, priors) \propto$$

$$\prod_{p=1}^{P} \prod_{m=1}^{M} \prod_{t=1}^{T} \mathrm{N}(q_{p,m,t} | \mathrm{f}(\boldsymbol{\theta}, \mathrm{FR_p}), \gamma_m + \rho_m \mathrm{f}(\boldsymbol{\theta}, \mathrm{FR_p}))$$

$$\prod_{p=1}^{P} \prod_{m=1}^{M} \prod_{t=1}^{T} \mathrm{N}(y_{p,m,t} | q_{p,m,t}, \tau^2_{p,m,t})$$

$$\prod_{p=1}^{P} p(FR_p) \prod_{f=1}^{F} p(\theta_f) \prod_{m=1}^{M} p(\gamma_m) \prod_{m=1}^{M} p(\rho_m)$$

Equation 7

where bolded components represent vectors, P is the total number of plots, M is the total number of data streams, T is the total months with observations, and F is the total number of 3-PG parameters that are optimized.

We numerically estimated the joint posterior distribution using the Monte-Carlo Markov Chain – Metropolis Hasting (MCMC-MH) algorithm (Zobitz et al., 2011). This approach has been widely used to approximate parameter distributions in ecosystem DA research (Fox et al., 2009; Trudinger et al., 2007; Williams et al., 2005; Zobitz et al., 2011). Briefly, the algorithm proposed

new values for the model parameters, uncertainty parameters, latent states, and FR. The proposed values were generated using a random draw from a normal distribution with a mean equal to the previously accepted value for that parameter and standard deviation equal to the parameter-specific jumping size. The ratio of the proposed calculation of Equation 7 to the previously accepted calculation of Equation 7 was used to determine if the proposed parameter was accepted. If the ratio was greater than or equal to 1 the proposed value was always accepted. If the ratio was less than 1, a random number between 0 and 1 was drawn and the proposed value was accepted if the ratio was greater than the random number. This allowed less probable parameter sets to be accepted, thus sampling the posterior distribution. We adapted the size of the jump size for each parameter to ensure the acceptance rate of the parameter set was between 22% and 43% (Ziehn et al., 2012) by adjusting the jump size if the acceptance rate for a parameter was outside the 22 – 43% range. All MCMC-MH chains were run for 30 million iterations with the first 15 million iterations discarded as the burn-in. Four chains were run and tested for convergence using the Gelman–Rubin convergence criterion, where a value for the criterion less than 1.1 indicated an acceptable level of convergence. We sampled every 1000th parameter in the final 15 million iterations of the MCMC-MH chain and used this thinned chain in the analysis described below. The 3-PG model and MCMC-MH algorithm were programed in FORTRAN 90 and used OpenMP to parallelize the simulation of each plot within an iteration of the MCMC-MH algorithm.

2.4 Data assimilation evaluation

Using the observations, model, and hierarchical Bayesian method described above, we assimilated both the non-manipulated and manipulated plots (Base assimilation; Table 4). We

assessed model performance first by calculating the RMSE and bias of stem biomass predictions (the most common data stream). In the evaluation, we only used the most recent observed values to increase the time length between initialization and validation. Second, we assessed the predictive capacity by comparing model predictions to data not used in the parameter optimization in a cross-validation study. In this evaluation, we repeated the Base assimilation without 160 FMRC thinning study plots (Table 2), predicted the 160 plots using the median parameter values, and calculated the RMSE and bias stem biomass of the independent set of plots. Rather than holding out all 160 plots from a single assimilation and not generating a converged chain, we divided the 160 plots into four unique sets of 40 plot and repeated the assimilation for each set. Finally, we compared the predicted responses to experimental manipulation to the observed responses. We focused the comparison on the percentage difference in stem biomass between the control and treatment plots. We used a paired t-test to test for differences between the predicted and observed responses within an experimental type (irrigated, drought, nutrient addition, and elevated CO_2). We combined the single and multi-factor treatments for analysis. For the analysis of the nutrient addition studies we only used plots where FR was assumed to be 1 so that we were able to simulate the treatments without requiring the optimization of a site-specific FR parameter.

During preliminary analysis, we found that the Base assimilation predicted lower stem biomass than observed in the elevated CO_2 plots in the Duke FACE study. Further analysis investigating the cause of the bias in the CO_2 plots showed that three parameters (wSx1000, ThinPower, and pCRS) were required to be unique to the Duke FACE study in order to reduce the bias. Therefore, the Base assimilation included unique parameters for wSx1000, ThinPower, and

pCRS parameters in all plots in the Duke FACE and US-DK3 studies. To highlight the need for the site-specific parameters, we repeated the Base assimilation approach without the three additional parameters for the Duke studies (NoDkPars assimilation).

2.5 Sensitivity to inclusion of ecosystem experiments

We also evaluated how parameter distributions and the associated environmental sensitivity of model predictions depended on the inclusion of ecosystem experiments in data assimilation. First, we repeated the Base assimilation, this time excluding the plots that included the manipulated treatments (NoExp). We removed all manipulation types at once, rather than individual experimental types, because all experimental types involved multi-factor studies. The NoExp assimilation had the same number of data streams as the Base assimilation because it included the control treatments from the experimental studies. The NoExp assimilation represented the situation where only observations across environmental gradients were available. Second, we compared the parameterization of the ASW, soil fertility, and atmospheric CO_2 environmental modifiers from the Base to the NoExp assimilation. The modifiers equations are described in Supplemental Material Section 1.2 and 1.3. Third, we repeated the same independent validation exercise for the 160 FMRC plots as described above for the Base assimilation. Fourth, we predicted the treatment plots in the irrigated, drought, nutrient addition (only plots where FR was assumed to be 1), and elevated CO_2 plots. As for the Base assimilation, we used a t-test to compare the experimental response between the NoExp assimilation and observed and between the NoExp and Base assimilations. Since the experimental treatments were not used in the optimization, this was an independent evaluation of predictive capacity.

450

451 **2.6 Regional predictions with uncertainty**

452 To demonstrate the capacity of the data assimilation system to create regional predictions with
453 uncertainty, we simulated the regional response to a decrease in precipitation, an increase in
454 nutrient availability, and an increase in atmospheric CO_2 concentration, each as a single factor
455 change from a 1985-2011 baseline. Each prediction included uncertainty by integrating across
456 the parameter posterior distributions using a Monte-Carlo sample of the parameter chains. Our
457 region corresponded to the native range of loblolly pine and used the HUC12 (USGS 12-digit
458 Hydrological Unit Code) watershed as the scale of simulation. For each HUC12 in the region we
459 used the mean SI, 30-year mean annual temperature, ASW aggregated to the HUC12 level, and
460 monthly meteorology from Abatzoglou (2013) as inputs (Figure 3). The SI of each HUC12 was
461 estimated from biophysical variables in the HUC12 using the method described in Sabatia and
462 Burkhart (2014). This SI corresponded to an estimated SI for stands without intensive
463 silvicultural treatments or advanced genetics of planted stock.

464

465 To sample parameter uncertainty, we randomly drew 500 samples from the Base assimilation
466 MCMC chain and simulated forest development from a 1985 planting to age 25 in 2011 in each
467 HUC. We chose age 25 as the final age because it is a typical age of harvest in the region. For
468 each sample, we repeated the regional simulation with 1) a 30% reduction in precipitation, 2) FR
469 set to 1, and 3) atmospheric CO_2 increased by 200 ppm. Within a parameter sample, we
470 calculated the percent change in stem biomass at age 25 between control simulation and the three
471 simulations with the environmental changes. We focused our regional analysis on the
472 distribution of the percent change in stem biomass.

3 Results

3.1 Data assimilation evaluation

Our multi-site, multi-experiment, multi-data stream DA approach (Base assimilation) increased confidence in the model parameters (Table 5). Averaged across parameters, the posterior 99% quantile range from the Base assimilation was 60% less than the prior range. The largest reduction in parameter uncertainty was for the parameters associated with light-use efficiency (alpha) and the conversion of GPP to NPP (y), which on average had ranges that were 85% lower in the posterior than the prior. Parameters associated with allocation and allometry had a 63% reduction in the range while parameters associated with mortality processes had 70% reduction in the range. Parameters associated with environmental modifiers had the least reduction in the range with a 40% decrease. In addition to the parameters associated with the 3-PG model, the model process error parameters for each data stream were well constrained with large reductions in the range (> 99% decrease; Supplemental Material Table 2)

The Base assimilation reliably predicted data from the regionally distributed non-manipulated plots that were not used in the optimization. The mean bias in stem biomass of the cross-validation was -3.7 % and the RMSE was 21.8 Mg ha^{-1} (Figure 4a). Furthermore, the response of stem biomass to irrigation ($df = 7$, $p = 0.18$), nutrient addition ($df = 26$, $p = 0.29$), and elevated CO_2 ($df = 4$, $p = 0.43$) was not significantly different between the observed and the Base assimilation (Figure 5). The Base assimilation was significantly more sensitive to drought than observed ($n = 31$, $p < 0.001$; Figure 5).

The plots at the Duke Forest study had a higher carrying capacity of stem biomass before self-thinning (WSx1000), smaller self-thinning parameter (ThinPower), and lower allocation to coarse root (pCRS) than values optimized from the other plots across the region (Table 6). The DA approach without these three study specific parameters (NoDkPars) predicted significantly lower accumulation of stem biomass in response to elevated CO_2 than observed ($df = 4$, $p = 0.002$; Figure 5). The NoDKPars assimilation optimized the CO_2 fertilization parameter (fCalpha700) to a value that predicted 45% less light-use efficiency at 700 ppm (1.13 in NoDKPar vs. 1.33 in Base; Table 6) than the Base assimilation.

3.2 **Sensitivity to inclusion of ecosystem experiments**

Excluding the experimental treatments from the data assimilation did not strongly influence the predictive capacity of the model. The RMSE validation plots in NoExp assimilation decreased slightly compared to Base assimilation (21.8 to 18.0 Mg ha^{-1}) while the bias slightly increased (-3.7 to -4.1%)(Figure 4b). Excluding the experimental treatments resulted in a significantly lower response of stem biomass to elevated CO_2 than observed ($df = 4$, $p < 0.001$; Figure 5). Furthermore, there was a slight negative response of stem biomass to CO_2 in the NoExp assimilation because the parameter governing the change in foliage allocation at elevated CO_2 (fCpFS700) was unconstrained by observations (Table 6). This led to convergence on the lower bound of the prior distribution (0.5) where foliage allocation decreased with increased atmospheric CO_2. The predictions of irrigation, drought, and nutrient addition experiments were not significantly different between the Base and NoExp assimilations (Figure 5).

519 The parameters and associated response functions in the 3-PG for nutrients, ASW, and
520 atmospheric CO_2 differed between the Base and NoExp assimilations (Figure 6). First, the
521 parameterization of the soil fertility rating (FR) showed a stronger dependence on SI in the
522 NoExp assimilation than in the Base assimilation (Figure 6a). For a given SI there was a lower
523 FR, thus stronger nutrient limitation, when experimental treatments were excluded from
524 assimilation. Second, the parameterization of the function relating photosynthesis and canopy
525 conductance to ASW resulted in lower photosynthesis and maximum conductance when soil
526 available water was less than 50% in the NoExp than Base assimilations (Figure 6b). Finally, the
527 response of photosynthesis to atmospheric CO_2 was functionally zero in the NoExp assimilation,
528 thus highlighting the importance of the elevated CO_2 treatments in the Duke FACE study for
529 constraining the parameterization of the CO_2 response function (Figure 6c).
530
531 **3.3 Regional predictions with uncertainty**
532 Regionally (i.e., the native range of loblolly pines), stem biomass at age 25 ranged from 52 Mg
533 ha^{-1} to 292 Mg ha^{-1} with the most productive areas located in the coastal plains and the interior of
534 Mississippi and Alabama (Figure 7a). The least productive locations were the western and
535 northern extents of the native range. The width of the 95% quantile interval for each HUC12 unit
536 ranged from 6.2 to 29.8 Mg ha^{-1} with largest uncertainty located in most the productive HUC12
537 units and in the far western extent of the region (Figure 7b).
538
539 The predicted change in stem biomass at age 25 from an additional 200 ppm of atmospheric CO_2
540 (over the 1985-2011 concentrations) was similar to the change associated with a removal of
541 nutrient limitation (by setting FR = 1) (Figure 8a,c). The median change associated with

elevated CO_2 for a given HUC12 unit ranged from 19.2 to 55.7% with a regional median of 21.7% (Figure 8a). The change associated the removal of nutrient limitation ranged from 6.9 to 303.7% for a given HUC12 unit, with regional median of 24.1% (Figure 8b). The response to elevated CO_2 was more consistent across space than the response to nutrient addition. The largest potential gains in productivity from nutrient addition were predicted in central Georgia, the northern extent of the region, and the western extents, areas with the lowest SI (Figure 3).

Stem biomass was considerably less responsive to a 30% decrease in precipitation, than to nutrient addition and an increase in atmospheric CO_2. The median change in stem biomass when precipitation was reduced from the 1985-2011 levels ranged from -11.6 to – 0.1% for a given HUC12 unit with a regional median of -5.1% (Figure 8c). Central Georgia was the most responsive to precipitation reduction reflecting the relatively low annual precipitation and warm temperatures (Figure 3).

For a given location, the predicted response to elevated CO_2 had larger uncertainty than the predicted response to precipitation reduction and nutrient limitation removal (Figure 8c,d,f). The uncertainty, defined as the width of the 95% quantile interval, was consistent across the region for the response to elevated CO_2 (Figure 8b). The uncertainty in the response to precipitation reduction and nutrient limitation removal was largest in the regions with the largest predicted change (Figure 8df).

4 Discussion

Using DA to parameterize models for predicting ecosystem change requires disentangling the

565 vegetation responses to temperature, precipitation, nutrients, and elevated CO_2. To address this
566 challenge, we introduced a regional-scale hierarchical Bayesian approach (DAPPER) that
567 assimilated data across environmental gradients and ecosystem manipulation experiments into a
568 modified version of the 3-PG model. Furthermore, we synthesized observations of carbon stocks,
569 carbon fluxes, water fluxes, vegetation structure, and vegetation dynamics that spanned 35 years
570 of forest research in a region (Table 1, Figure 1) with large and dynamic carbon fluxes (Lu et al.,
571 2015). By combining the DAPPER system with the regional set of observations, we were able to
572 estimate parameters in a model with high predictive capacity (Figure 4) and with quantified
573 uncertainty on parameters (Table 5) and regional simulations (Figures 7 and 8).
574
575 Our hierarchical approach (Equation 7) was designed to partition uncertainty among parameters,
576 model process, and measurements (Hobbs and Hooten, 2015). Separating the parameter and
577 process uncertainty is required to estimate prediction intervals, as prediction intervals only
578 include parameter and process errors (Dietze et al., 2013; Hobbs and Hooten, 2015). Previous
579 forest ecosystem DA efforts have either focused on parameter uncertainty, by using
580 measurement uncertainty as the variance term in a Gaussian cost function (Bloom and Williams,
581 2015; Keenan et al., 2012; Richardson et al., 2010) or on total uncertainty by directly estimating
582 the Gaussian variance term (Ricciuto et al., 2008). Our approach allowed the estimation of the
583 probability distribution of forest biomass before uncertainty is added through measurement.
584 Considering that the method of DA can potentially have a large influence on posterior parameter
585 distributions (Trudinger et al., 2007), future research should focus on comparing the hierarchical
586 approach presented here to other approaches by using the same data constraints with alternative
587 cost functions.

588

589 **4.1 Sensitivity to inclusion of ecosystem experiments**

590 The most important experimental manipulation for constraining model parameters was the Duke
591 FACE CO_2 fertilization study because the CO_2 fertilization parameters (fCalpha700 and
592 fCpFS700) converged on the lower bounds of their prior distributions when the experiments
593 were excluded from the assimilation. In contrast, excluding the nutrient fertilization, drought,
594 and irrigation studies did not substantially alter the predictive capacity of the model. This
595 finding suggests that data assimilation using plots across environmental gradients alone can
596 constrain parameters associated with water and nutrient sensitivity. However, regardless of
597 whether the experiments were included in the assimilation, the optimized model predicted higher
598 sensitivity to drought than observed, highlighting that future studies should focus on improving
599 the sensitivity to drought.

600

601 The 3-PG model included a highly-simplified representation of interactions between the water
602 and carbon cycles that resulted in parameterizations that may contain assumptions that require
603 additional investigation. First, transpiration was modeled as a function of a potential canopy
604 transpiration that occurred if leaf area was not limiting transpiration. The LAI at which leaf area
605 was no longer limiting was a parameter that was optimized (LAIgcx in Table 5), resulting in a
606 value of 2.2. Interestingly, this optimized value is consistent with the scant literature on this
607 topic. In their analysis of multi-year measurements of transpiration in loblolly pine, Phillips and
608 Oren (2001) observed that transpiration per unit leaf area was relatively insensitive to increases
609 in leaf area above LAI of approximately 2.5. Iritz and Lindroth (1996) reviewed transpiration
610 data from a range of crop species and found only small increases in transpiration above LAI of 3-

4. These authors suggest that the threshold-type responses observed were related to the range of LAI at which self-shading increases most rapidly, therefore limiting increases in transpiration. The resulting model behavior of "flat" transpiration above 2.2 LAI, with gradually decreasing photosynthesis above that value, results in increasing water use efficiency at higher LAI values. Second, the relationship between relative ASW and the modifier of photosynthesis and transpiration predicted a modifier value greater than zero when the relative ASW was zero. This resulted in positive values from photosynthesis and transpiration when the average ASW during the month was zero. In practice, the monthly ASW was rarely zero during simulations, which presents a challenge constraining the shape of the ASW modifier. The priors for the two ASW modifiers (SWconst and SWpower) had ranges that permitted the modifier to be zero. Therefore, additional data are likely needed during very dry conditions to develop a more physically based parameterization. Alternatively, the parameterization of a non-zero soil moisture modifier at zero ASW may be due to trees having access to water at soil depths deeper than the top 1.5 m of soil represented by the bucket in 3-PG. Overall, it is important to view the parameterization presented here as a phenomenological relationship that is consistent with observations from drought and irrigation experiments as well as observations across regional gradients in precipitation.

Constraining the sensitivity to atmospheric CO_2 differs from constraining the sensitivity to ASW because, unlike the multiple constraints on water sensitivity (drought, irrigation, and gradient studies), environmental conditions created by the few elevated CO_2 plots provided unique constraint on parameters. Our finding demonstrated that DA efforts should test for bias in unique ecosystem experiments before finalizing a set of model parameters used in optimization. In particular, we found that the parameter governing the photosynthetic response to elevated CO_2

(fCalpha700) was substantially lower when all parameters were assumed to be shared across all plots than when the CO_2 fertilization experiment was allowed to have unique parameters. The need for the three unique parameters at the Duke FACE study parameters can be explained by the constraint provided by multiple data streams and multiple plots. An assumption of the model was that an increase in stem biomass caused a decrease stem density through self-thinning, unless the average tree stem biomass was below a parameterized threshold (WSx1000). Therefore, an increase in photosynthesis and stem biomass through CO_2 fertilization could cause a decrease in stem density. For a single study, it is straightforward to simultaneously fit the CO_2 fertilization and self-thinning parameters to fit stem biomass and stem density observations for the site. However, regional DA presents a challenge because the self-thinning parameters are well constrained by the stem biomass and stem density observations across the region but the CO_2 fertilization parameters are not. As a result of the regional DA, the self-thinning parameters caused a stronger decrease in stem density than observed in the Duke FACE study. Therefore, the optimization favored a solution where there was a lower response to CO_2, thus a smaller decrease in stem density. Allowing the Duke FACE study to have unique self-thinning parameters that resulted in lower rates of self-thinning and allowed for simulated stem biomass to respond to CO_2 in a way that matched the observations without penalizing the optimization by degrading the fit to the stem density.

Our finding that the Duke FACE study required unique self-thinning parameters to reduce bias in the simulated stem biomass suggests that when using DA to optimize parameters that are shared across plots, careful examination of prediction bias in key sites that provide unique constraint on certain parameters (like the Duke FACE) is critical. Based on this example, we suggest that DA

efforts using multiple studies and multiple experiment types identify whether particular experiments at limited number of sites have the potential to uniquely constrain specific parameters. In this case, additional weight or site-specific parameters may be needed to avoid having the signal of the unique experiment overwhelmed by the large amount of data from the other sites and experiments. Additionally, the finding suggests that multi-site DA should consider using hierarchical approaches to predicting mortality, particularly because mortality is often not simulated as mechanistically as growth. A hierarchical approach, where each plot has a set of mortality parameters that are drawn from a regional distribution, could avoid having unexplained variation in mortality rates lead to bias in the parameterization of growth related processes (i.e., growth responses to CO_2, drought, nutrient fertilization, etc.). The hierarchical approach to mortality could also highlight patterns in mortality rates across a region and allow for additional investigations in the mechanisms driving the patterns.

4.2 Regional predictions with uncertainty

Our predictions of how stem biomass responses to elevated CO_2, nutrient addition, and drought were designed to illustrate the capacity of the DAPPER approach to simulate the uncertainty in future predictions. By using DA, our regional predictions and the uncertainty are consistent with observations but are associated with key caveats. First, only parameter uncertainty was presented in the regional simulations. There is additional uncertainty associated with model process error. We showed the parameter uncertainty because it isolated the capacity to parameterize the individual environmental response functions in the model. Second, the response to drought may be too strong because of the bias in the model predictions of the drought studies. However, there is potential that the drought studies underestimated the

sensitivity to ASW since they are relatively short term (< 5 years) and manipulate local ASW without manipulating large scale ASW (i.e., regional water tables). Third, the large responses to N fertilization at the western and northern extents of the study region may be too high. The large responses are attributed to the low SI and the low predicted site fertility index (FR_p). The low SI may be attributable to water limitation and temperature limitation that is not fully accounted for in the parameterization. Additional nutrient addition experiments in the northern and western extent along with further development of the representation of nutrient availability in the 3-PG model may allow for a more robust representation of soil fertility. Finally, the baseline fertility used in our regional analysis was derived from an empirical model of SI that was developed using field plots with minimal management (Sabatia and Burkhart, 2014). Subsequently our estimate of baseline fertility is likely on the low end of forest stands currently in production and the response to nutrient addition may be higher than a typical stand under active management.

5 Conclusions

DA is increasingly used for developing predictions from ecosystem models that include uncertainty estimation, due to its ability represent prior knowledge, integrate observations into the parameterization, and estimate multiple components of uncertainty, including observation, parameter, and process representation uncertainty (Dietze et al., 2013; Luo et al., 2011; Niu et al., 2014). Our application of DA to loblolly pine plantations of the southeastern U.S demonstrated that these ecosystems are well suited as a test-bed for the development of DA techniques, particularly techniques for assimilating ecosystem experiments. We found that assimilating observations across environmental gradients can provide substantial constraint on many model parameters but that ecosystem manipulative experiments, particularly elevated CO_2

studies, were critical for constraining parameters associated forest productivity in a more CO_2 enriched atmosphere. This highlights the importance of whole-ecosystem manipulation CO_2 experiments for helping to parameterize and evaluate ecosystem models. Finally, we present an approach for the development of future predictions of forest productivity for natural resource managers that leverage a rich dataset of integrated ecosystem observations across a region.

6 Data availability

Observations used in the DA can be found in the following: Duke FACE study can be found in McCarthy et al. (2010), the PINEMAP studies are available through the TerraC database (http://terrac.ifas.ufl.edu), the US-DK3 eddy-flux tower data are available through the Ameriflux database (http://ameriflux-data.lbl.gov), the Waycross data can be found in Bryars et al. (2013), the US-NC2 data are available upon request from Asko Noormets, the FMRC and FPC are available through membership with the cooperatives. The parameter chains and 3-PG model code are available upon request from R. Quinn Thomas.

Acknowledgments

Funding support came from USDA-NIFA Project 2015-67003-23485 and the Pine Integrated Network: Education, Mitigation, and Adaptation project (PINEMAP), a Coordinated Agricultural Project funded by the USDA National Institute of Food and Agriculture, Award #2011-68002-30185. Additional funding support came from USDA-NIFA McIntire-Stennis Program. The Virginia Space Grant Consortium Graduate STEM Research Fellowship Program provided partial support for A. Jersild. Computational support was provided by Virginia Tech Advanced Research Computing. This research was also supported by grants from the French

Research Agency (MACACC ANR-13-AGRO-0005 and MARIS ANR-14-CE03-0007). We thank Luke Smallman and Mat Williams for helpful discussions about data assimilation, the corporate and government agency members of the FPC and FMRC research cooperatives for supporting the extensive long-term experimental and observational plots in those datasets, and Anthony Walker and an anonymous reviewer for helpful feedback on the manuscript. This material is based upon work supported by the U.S. Department of Energy, Office of Science, Office of Biological and Environmental Research, under contract number DE-AC05-00OR22725.

References

Abatzoglou, J. T.: Development of gridded surface meteorological data for ecological applications and modelling, International Journal of Climatology, 33(1), 121–131, doi:10.1002/joc.3413, 2013.

Albaugh, T. J., Albaugh, J. M., Fox, T. R., Allen, H. L., Rubilar, R. A., Trichet, P., Loustau, D. and Linder, S.: Tamm Review: Light use efficiency and carbon storage in nutrient and water experiments on major forest plantation species, Forest Ecol Manag, 376, 333–342, doi:10.1016/j.foreco.2016.05.031, 2016.

Albaugh, T. J., Allen, H. L. and Kress, L. W.: Root and stem partitioning of *Pinus taeda*, Trees, 20(2), 176–185, doi:10.1007/s00468-005-0024-4, 2005.

Albaugh, T. J., Lee Allen, H., Dougherty, P. M. and Johnsen, K. H.: Long term growth responses of loblolly pine to optimal nutrient and water resource availability, Forest Ecol Manag, 192(1), 3–19, doi:10.1016/j.foreco.2004.01.002, 2004.

Albaugh, T., Fox, T., Allen, H. and Rubilar, R.: Juvenile southern pine response to fertilization is influenced by soil drainage and texture, Forests, 6(8), 2799–2819, doi:10.3390/f6082799, 2015.

Allen, C. B., Will, R. E. and Jacobson, M. A.: Production efficiency and radiation use efficiency of four tree species receiving irrigation and fertilization, Forest Science, 51(6), 556–569, 2005.

Bartkowiak, S. M., Samuelson, L. J., McGuire, M. A. and Teskey, R. O.: Fertilization increases sensitivity of canopy stomatal conductance and transpiration to throughfall reduction in an 8-year-old loblolly pine plantation, Forest Ecol Manag, 354, 87–96, doi:10.1016/j.foreco.2015.06.033, 2015.

757 Bloom, A. A. and Williams, M.: Constraining ecosystem carbon dynamics in a data-limited
758 world: integrating ecological "common sense" in a model–data fusion framework,
759 Biogeosciences, 12(5), 1299–1315, doi:10.5194/bg-12-1299-2015, 2015.

760 Bryars, C., Maier, C., Zhao, D., Kane, M., Borders, B., Will, R. and Teskey, R.: Fixed
761 physiological parameters in the 3-PG model produced accurate estimates of loblolly pine growth
762 on sites in different geographic regions, Forest Ecol Manag, 289, 501–514,
763 doi:10.1016/j.foreco.2012.09.031, 2013.

764 Burkhart, H. E., Cloeren, D. C. and Amateis, R. L.: Yield relationships in unthinned loblolly pine
765 plantations on cutover, site-prepared lands, Southern Journal of Applied Forestry, 9(2), 84–91,
766 1985.

767 Carlson, C. A., Fox, T. R., Allen, H. L., Albaugh, T. J., Rubilar, R. A. and Stape, J. L.: Growth
768 responses of loblolly pine in the Southeast United States to midrotation applications of nitrogen,
769 phosphorus, potassium, and micronutrients, Forest Science, 60(1), 157–169,
770 doi:10.5849/forsci.12-158, 2014.

771 DeLucia, E. H., Drake, J. E., Thomas, R. B. and Gonzalez-Meler, M.: Forest carbon use
772 efficiency: is respiration a constant fraction of gross primary production? Global Change
773 Biology, 13(6), 1157–1167, doi:10.1111/j.1365-2486.2007.01365.x, 2007.

774 Dieguez-Aranda, U., Burkhart, H. E. and Amateis, R. L.: Dynamic site model for loblolly pine
775 (*Pinus taeda L.*) plantations in the United States, Forest Science, 52(3), 262–272, 2006.

776 Dietze, M. C., LeBauer, D. S. and Kooper, R.: On improving the communication between
777 models and data, Plant Cell Environ, 36(9), 1575–1585, doi:10.1111/pce.12043, 2013.

778 Ewers, B. E., Oren, R., Phillips, N., Stromgren, M. and Linder, S.: Mean canopy stomatal
779 conductance responses to water and nutrient availabilities in Picea abies and Pinus taeda, Tree
780 Physiology, 21(12-13), 841–850, 2001.

781 Fox, A., Williams, M., Richardson, A. D., Cameron, D., Gove, J. H., Quaife, T., Ricciuto, D.,
782 Reichstein, M., Tomelleri, E., Trudinger, C. M. and Van Wijk, M. T.: The REFLEX project:
783 Comparing different algorithms and implementations for the inversion of a terrestrial ecosystem
784 model against eddy covariance data, Agr Forest Meteorol, 149(10), 1597–1615,
785 doi:10.1016/j.agrformet.2009.05.002, 2009.

786 Fox, T. R., Jokela, E. J. and Allen, H. L.: The development of pine plantation silviculture in the
787 Southern United States, Journal of Forestry, 105(7), 337–347, 2007.

788 Gonzalez-Benecke, C. A. and Martin, T. A.: Water availability and genetic effects on water
789 relations of loblolly pine (*Pinus taeda*) stands, Tree Physiology, 30(3), 376–392,
790 doi:10.1093/treephys/tpp118, 2010.

791 Gonzalez-Benecke, C. A., Gezan, S. A., Albaugh, T. J., Allen, H. L., Burkhart, H. E., Fox, T. R.,
792 Jokela, E. J., Maier, C. A., Martin, T. A., Rubilar, R. A. and Samuelson, L. J.: Local and general
793 above-stump biomass functions for loblolly pine and slash pine trees, Forest Ecol Manag, 334,

254–276, doi:10.1016/j.foreco.2014.09.002, 2014.

Gonzalez-Benecke, C. A., Teskey, R. O., Martin, T. A., Jokela, E. J., Fox, T. R., Kane, M. B. and Noormets, A.: Regional validation and improved parameterization of the 3-PG model for *Pinus taeda* stands, Forest Ecol Manag, 361, 237–256, doi:10.1016/j.foreco.2015.11.025, 2016.

Hobbs, N. T. and Hooten, M. B.: Bayesian Models: A Statistical Primer for Ecologists, Princeton University Press, Princeton. 2015.

Iritz, Z. and Lindroth, A.: Energy partitioning in relation to leaf area development of short-rotation willow coppice, Agr Forest Meteorol, 81(1-2), 119–130, doi:10.1016/0168-1923(95)02306-2, 1996.

Keenan, T. F., Carbone, M. S., Reichstein, M. and Richardson, A. D.: The model–data fusion pitfall: assuming certainty in an uncertain world, Oecologia, 167(3), 587–597, doi:10.1007/s00442-011-2106-x, 2011.

Keenan, T. F., Davidson, E., Moffat, A. M., Munger, W. and Richardson, A. D.: Using model-data fusion to interpret past trends, and quantify uncertainties in future projections, of terrestrial ecosystem carbon cycling, Global Change Biology, 18(8), 2555–2569, doi:10.1111/j.1365-2486.2012.02684.x, 2012.

Landsberg, J. and Waring, R.: A generalised model of forest productivity using simplified concepts of radiation-use efficiency, carbon balance and partitioning, Forest Ecol Manag, 95(3), 209–228, doi:10.1016/S0378-1127(97)00026-1, 1997.

Le Quere, C., Moriarty, R., Andrew, R. M., Canadell, J. G., Sitch, S., Korsbakken, J. I., Friedlingstein, P., Peters, G. P., Andres, R. J., Boden, T. A., Houghton, R. A., House, J. I., Keeling, R. F., Tans, P., Arneth, A., Bakker, D. C. E., Barbero, L., Bopp, L., Chang, J., Chevallier, F., Chini, L. P., Ciais, P., Fader, M., Feely, R. A., Gkritzalis, T., Harris, I., Hauck, J., Ilyina, T., Jain, A. K., Kato, E., Kitidis, V., Klein Goldewijk, K., Koven, C., Landsch utzer, P., Lauvset, S. K., Lef evre, N., Lenton, A., Lima, I. D., Metzl, N., Millero, F., Munro, D. R., Murata, A., Nabel, J. E. M. S., Nakaoka, S., Nojiri, Y., O'Brien, K., Olsen, A., Ono, T., P 'erez, F. F., Pfeil, B., Pierrot, D., Poulter, B., Rehder, G., R odenbeck, C., Saito, S., Schuster, U., Schwinger, J., S 'ef 'erian, R., Steinhoff, T., Stocker, B. D., Sutton, A. J., TAKAHASHI, T., Tilbrook, B., van der Laan-Luijkx, I. T., van der Werf, G. R., van Heuven, S., Vandemark, D., Viovy, N., Wiltshire, A., Zaehle, S. and Zeng, N.: Global Carbon Budget 2015, Earth Syst. Sci. Data, 7(2), 349–396, doi:10.5194/essd-7-349-2015, 2015.

LeBauer, D. S., Dietze, M., Long, S., Mulrooney, P., Rohde, G. S., Wang, D. and Kooper, R.: *Biofuel Ecophysiological Traits and Yields Database (BETYdb)*,, doi:doi:10.13012/J8H41PB9, 2010.

Lu, X., Lu, X., Kicklighter, D. W., Kicklighter, D., Melillo, J. M., Melillo, J. M., Reilly, J. M., Reilly, J. M., Xu, L. and Wu, L.: Land carbon sequestration within the conterminous United States: Regional- and state-level analyses, J Geophys Res-Biogeo, 120(2), 379–398, doi:10.1002/2014JG002818, 2015.

832 Luo, Y., Ogle, K., Tucker, C., Fei, S., Gao, C., LaDeau, S., Clark, J. S. and Schimel, D. S.:
833 Ecological forecasting and data assimilation in a data-rich era, Ecological Applications, 21(5),
834 1429–1442, doi:10.1890/09-1275.1, 2011.

835 Luo, Y., Weng, E., Wu, X., Gao, C., Zhou, X. and Zhang, L.: Parameter identifiability,
836 constraint, and equifinality in data assimilation with ecosystem models, Ecological Applications,
837 19(3), 571–574, doi:10.1890/08-0561.1, 2009.

838 MacBean, N., Peylin, P., Chevallier, F., Scholze, M. and Schürmann, G.: Consistent assimilation
839 of multiple data streams in a carbon cycle data assimilation system, Geosci. Model Dev., 9(10),
840 3569–3588, doi:10.5194/gmd-9-3569-2016, 2016.

841 Matamala, R., Gonzàlez-Meler, M. A., Jastrow, J. D., Norby, R. J. and Schlesinger, W. H.:
842 Impacts of fine root turnover on forest NPP and soil C sequestration potential, Science,
843 302(5649), 1385–1387, doi:10.1126/science.1089543, 2003.

844 McCarthy, H. R., Oren, R., Johnsen, K. H., Gallet-Budynek, A., Pritchard, S. G., Cook, C. W.,
845 LaDeau, S. L., Jackson, R. B. and Finzi, A. C.: Re-assessment of plant carbon dynamics at the
846 Duke free-air CO_2 enrichment site: interactions of atmospheric [CO_2] with nitrogen and water
847 availability over stand development, New Phytol, 185(2), 514–528, doi:10.1111/j.1469-
848 8137.2009.03078.x, 2010.

849 McKeand, S., Mullin, T., Byram, T. and White, T.: Deployment of genetically improved loblolly
850 and slash pines in the south, Journal of Forestry, 101(3), 32–37, 2003.

851 Medlyn, B. E., Zaehle, S., De Kauwe, M. G., Walker, A. P., Dietze, M. C., Hanson, P. J.,
852 Hickler, T., Jain, A. K., Luo, Y., Parton, W., Prentice, I. C., Thornton, P. E., Wang, S., Wang,
853 Y.-P., Weng, E., Iversen, C. M., McCarthy, H. R., Warren, J. M., Oren, R. and Norby, R. J.:
854 Using ecosystem experiments to improve vegetation models, Nature Climate Change, 5(6), 528–
855 534, doi:10.1038/nclimate2621, 2015.

856 Niu, S., Luo, Y., Dietze, M. C., Keenan, T. F., Shi, Z., Li, J. and III, F. S. C.: The role of data
857 assimilation in predictive ecology, Ecosphere, 5(5), art65–16, doi:10.1890/ES13-00273.1, 2014.

858 Noormets, A., Gavazzi, M. J., McNulty, S. G., Domec, J.-C., Sun, G., King, J. S. and Chen, J.:
859 Response of carbon fluxes to drought in a coastal plain loblolly pine forest, Glob Change Biol,
860 16(1), 272–287, doi:10.1111/j.1365-2486.2009.01928.x, 2010.

861 Novick, K. A., Oishi, A. C., Ward, E. J., Siqueira, M. B. S., Juang, J.-Y. and Stoy, P. C.: On the
862 difference in the net ecosystem exchange of CO_2 between deciduous and evergreen forests in the
863 southeastern United States, Glob Change Biol, 21(2), 827–842, doi:10.1111/gcb.12723, 2015.

864 Oren, R., Ellsworth, D., Johnsen, K., Phillips, N., Ewers, B., Maier, C., Schafer, K., McCarthy,
865 H., Hendrey, G., McNulty, S. G. and Katul, G.: Soil fertility limits carbon sequestration by forest
866 ecosystems in a CO_2-enriched atmosphere, Nature, 411(6836), 469–472, doi:10.1038/35078064,
867 2001.

868 Pan, Y., Birdsey, R. A., Fang, J., Houghton, R., Kauppi, P. E., Kurz, W. A., Phillips, O. L.,

869 Shvidenko, A., Lewis, S. L., Canadell, J. G., Ciais, P., Jackson, R. B., Pacala, S. W., McGuire,
870 A. D., Piao, S. L., Rautiainen, A., Sitch, S. and Hayes, D.: A large and persistent carbon sink in
871 the world's forests, Science, 333(6045), 988–993, doi:10.1126/science.1201609, 2011.

872 Phillips, N. and Oren, R.: Intra- and inter-annual variation in transpiration of a pine forest,
873 Ecological Applications, 11(2), 385–396, 2001.

874 Raymond, J. E., Fox, T. R., Strahm, B. D. and Zerpa, J.: Differences in the recovery of four
875 different nitrogen containing fertilizers after two application seasons in pine plantations across
876 the southeastern United States, Forest Ecol Manag, 380(C), 161–171,
877 doi:10.1016/j.foreco.2016.08.044, 2016.

878 Ricciuto, D. M., Davis, K. J. and Keller, K.: A Bayesian calibration of a simple carbon cycle
879 model: The role of observations in estimating and reducing uncertainty, Global Biogeochem.
880 Cycles, 22(2), GB2030, doi:10.1029/2006GB002908, 2008.

881 Richardson, A. D., Williams, M., Hollinger, D. Y., Moore, D. J. P., Dail, D. B., Davidson, E. A.,
882 Scott, N. A., Evans, R. S., Hughes, H., Lee, J. T., Rodrigues, C. and Savage, K.: Estimating
883 parameters of a forest ecosystem C model with measurements of stocks and fluxes as joint
884 constraints, Oecologia, 164, 25–40, doi:10.1007/s00442-010-1628-y, 2010.

885 Sabatia, C. O. and Burkhart, H. E.: Predicting site index of plantation loblolly pine from
886 biophysical variables, Forest Ecol Manag, 326, 142–156, doi:10.1016/j.foreco.2014.04.019,
887 2014.

888 Samuelson, L. J., Butnor, J., Maier, C., Stokes, T. A., Johnsen, K. and Kane, M.: Growth and
889 physiology of loblolly pine in response to long-term resource management: defining growth
890 potential in the southern United States, Can. J. For. Res., 38(4), 721–732, doi:10.1139/X07-191,
891 2008.

892 Shvidenko, A., Barber, C. V. and Persson, R.: Forest and Woodland Systems, in Ecosystems and
893 Human Well-being Current State and Trends, Volume, edited by R. Hassan, R. Scholes, and N.
894 Ash, pp. 585–621, Island Press, Washington. 2005.

895 Soil Survey Staff, Natural Resources Conservation Service, United States Department of
896 Agriculture. Soil Survey Geographic (SSURGO) Database. Available online
897 at https://sdmdataaccess.sc.egov.usda.gov. Accessed 11/12/2013
898
899 Subedi, S., Fox, T. and Wynne, R.: Determination of fertility rating (FR) in the 3-PG model for
900 loblolly pine plantations in the Southeastern United States based on site index, Forests, 6(9),
901 3002–3027, doi:10.3390/f6093002, 2015.

902 Tang, Z., Sayer, M. A. S., Chambers, J. L. and Barnett, J. P.: Interactive effects of fertilization
903 and throughfall exclusion on the physiological responses and whole-tree carbon uptake of mature
904 loblolly pine, Canadian Journal of Botany, 82(6), 850–861, doi:10.1139/b04-064, 2004.

905 Trudinger, C. M., Raupach, M. R., Rayner, P. J., Kattge, J., Liu, Q., Pak, B., Reichstein, M.,
906 Renzullo, L., Richardson, A. D., Roxburgh, S. H., Styles, J., Wang, Y.-P., Briggs, P., Barrett, D.

907 and Nikolova, S.: OptIC project: An intercomparison of optimization techniques for parameter
908 estimation in terrestrial biogeochemical models, J. Geophys. Res., 112(G2), G02027–17,
909 doi:10.1029/2006JG000367, 2007.

910 Ward, E. J., Domec, J.-C., Laviner, M. A., Fox, T. R., Sun, G., McNulty, S., King, J. and
911 Noormets, A.: Fertilization intensifies drought stress: Water use and stomatal conductance of
912 Pinus taeda in a midrotation fertilization and throughfall reduction experiment, Forest Ecol
913 Manag, 355, 72–82, doi:10.1016/j.foreco.2015.04.009, 2015.

914 Weng, E. and Luo, Y.: Relative information contributions of model vs. data to short- and long-
915 term forecasts of forest carbon dynamics, Ecological Applications, 21(5), 1490–1505,
916 doi:10.1890/09-1394.1, 2011.

917 Will, R., Fox, T., Akers, M., Domec, J.-C., González-Benecke, C., Jokela, E., Kane, M., Laviner,
918 M., Lokuta, G., Markewitz, D., McGuire, M., Meek, C., Noormets, A., Samuelson, L., Seiler, J.,
919 Strahm, B., Teskey, R., Vogel, J., Ward, E., West, J., Wilson, D. and Martin, T.: A range-wide
920 experiment to investigate nutrient and soil moisture interactions in loblolly pine plantations,
921 Forests, 6(6), 2014–2028, doi:10.3390/f6062014, 2015.

922 Williams, M., Schwarz, P., Law, B. E., Irvine, J. and Kurpius, M.: An improved analysis of
923 forest carbon dynamics using data assimilation, Global Change Biology, 11(1), 89–105,
924 doi:10.1111/j.1365-2486.2004.00891.x, 2005.

925 Zobitz, J. M., Desai, A. R., Moore, D. J. P. and Chadwick, M. A.: A primer for data assimilation
926 with ecological models using Markov Chain Monte Carlo (MCMC), Oecologia, 167(3), 599–
927 611, doi:10.1007/s00442-011-2107-9, 2011.

928

929

930

Table 1. Regional observational data streams used in data assimilation.

Data stream	Measurement frequency	Measurement or estimation technique	Uncertainty	Stream ID for Table 3
Foliage biomass (Pine)	Annual or less	Allometric relationship	Based on propagating the allometric model uncertainty in Gonzalez-Benecke et al. 2014. Varied by observation.	1
Foliage biomass (hardwood)	Annual or less	Allometric relationship	Assumed zero	2
Stem biomass (pine)	Annual or less	Allometric relationship	Based on propagating the allometric model uncertainty in Gonzalez-Benecke et al. 2014. Varied by observation.	3
Stem biomass (hardwood)	Annual or less	Allometric relationship	Assumed zero	4
Coarse root biomass (combined)	Annual or less	Allometric relationship	Assumed zero*	5
Fine root biomass (combined)	Annual or less	Allometric relationship	SD = 10% of observation	6
Foliage biomass production (combined)	Annual	Litterfall traps	SD = 10% of observation	7
Fine root biomass production (combined)	Annual	Mini-rhizotrons	SD = 10% of observation	8
Pine stem density	Annual or less	Counting individuals	1% (assumed small)	9
Leaf area index (pine)	Monthly to annual	Litter traps or LI 2000	SD = 10% of observation	10
Leaf area index (hardwood)	Monthly to annual	Litter traps or LI 2000	SD = 10% of observation	11
Leaf area index (combined)	Only used if not separated into pine and hardwood	Litter traps or LI 2000	SD = 10% of observation	12
Gross Ecosystem Production	Monthly	Modeled from flux eddy-covariance net	SD = 10% of observation	13

Evapotranspiration	Monthly	ecosystem exchange Eddy-covariance	SD = 10% of observation	14

*the relatively low number of observations prevented convergence when using the observational uncertainty model so observational uncertainty was assumed to be zero to allow convergence.

Table 2. Descriptions of the studies used in data assimilation.

Study name	Number of locations	Number of plots per site	Experimental treatments (plots)	Data streams (Table 2)	Measurement Years	Measurement Stand Ages (years)	Reference
FMRC[1] Thinning Study	163	1	None	1, 3,9	1981 - 2003	8 - 30	Burkhart et al. (1985)
FPC[2] Region-wide 18	18	2	Nutrient addition	1, 3,9	2011-2014	12-21	Albaugh et al. (2015)
PINEMAP[3]	4	16	Nutrient addition, 30% throughfall, Nutrient x throughfall	1, 3,9	2011-2015	3 – 13	Will et al. (2015)
Waycross	1	2	Nutrient addition	3,9,10	1991-2010	4-23	Bryars et al. (2013)
SETRES[4]	1	16	Nutrient addition, irrigation, nutrient x irrigation	1,3,5,6, 9,10	1991-2006	8 - 23	Albaugh et al. (2004)
Duke FACE[5] and US-DK3 Flux	1	12	CO_2, nutrient addition, CO_2 x nutrient addition	2,3,4,5, 6,7,8,9, 10,11,13,14	1996-2004	13-22	McCarthy et al. (2010); Novick et al. (2015)
NC2 Flux	1	1	None	2,3,4,5, 6,7,9,10,11,12,13,14	2005-2014	12-22	Noormets et al. (2010)
Total	187	294			1981 - 2014	4 - 30	

[1]Forest Modeling Research Cooperative; [2] Forest Productivity Cooperative; [3] Pine Integrated Network: Education, Mitigation, and Adaptation project (PINEMAP); [4] Southeast Tree Research

and Education Site; [5] Free Air Carbon Enrichment

938

Table 3. The prior distributions of all 3-PG model parameters optimized using data assimilation.

Parameter	Parameter description	Units	Prior distribution	Prior parameters	Reference for prior (see footnote)
Allocation and structure					
pFS2	Ratio of foliage to stem allocation at stem diameter = 2 cm	-	uniform	min = 0.08 max = 1.00	uninformed
pFS20	Ratio of foliage to stem allocation at stem diameter = 20 cm	-	uniform	min = 0.10 max =1.00	uninformed
pRF	Ratio of fine roots to foliage allocation	-	uniform	min = 0.05 max = 2.00	uninformed
pCRS	Ratio of coarse roots to stem allocation	-	uniform	min = 0.15 max = 0.35	1
SLA0	Specific leaf area at stand age 0	$m^2\ kg^{-1}$		mean =5.53 sd = 0.44	2
SLA1	Specific leaf area for mature aged stands	$m^2\ kg^{-1}$	normal	mean = 3.58 sd = 0.11	2
tSLA	Age at which specific leaf area = 0.5(SLA0 + SLA1)	Years	normal	mean = 5.97 sd = 2.15	2
fCpFS700	Proportional decrease in allocation to foliage between 350 and 700 ppm CO_2	-	uniform	min = 0.50 max = 1.00	uninformed
StemConst	Constant in stem mass vs. diameter relationship	-	normal	mean = 0.022 sd = 0.005	3
StemPower	Power in stem mass vs. diameter relationship	-	normal	mean = 2.77 sd = 0.2	3
Canopy photosynthesis, autotrophic respiration, and transpiration					
alpha	Canopy quantum efficiency (pines)	mol C mol PAR^{-1}	uniform	min = 0.02 max = 0.06	uninformed
y	Ratio NPP/GPP	-	uniform	min = 0.30 max= 0.65	4
MaxCond	Maximum canopy conductance	$m\ s^{-1}$	uniform	min = 0.005 max = 0.03	2
LAIgcx	Canopy LAI for maximum canopy conductance	-	uniform	min = 2 max = 5	2,5,6
Environmental modifiers of photosynthesis and transpiration					

kF	Reduction rate of production per degree Celsius below zero	-	normal	mean = 0.18 sd = 0.016	2
Tmin	Minimum monthly mean temperature for growth	°C	normal	mean = 4.0 sd = 2.0	2,5,6
Topt	Optimum monthly mean temperature for growth	°C	normal	mean = 25.0 sd = 2.0	2,5,6
Tmax	Maximum monthly mean temperature for growth	°C	normal	mean = 38.0 sd = 2.0	2,5,6
SWconst	Moisture ratio deficit when downregulation is 0.5	-	uniform	min = 0.01 max = 1.8	uninformed
SWpower	Power of moisture ratio deficit	-	uniform	min = 1 max= 13	uninformed
CoeffCond	Defines stomatal response to VPD	$mbar^{-1}$	normal	mean = 0.041 sd = 0.003	2
fCalpha700	Proportional increase in canopy quantum efficiency between 350 and 700 ppm CO_2	-	uniform	min = 1.00 max = 1.8	uninformed
MaxAge	Maximum stand age used to compute relative age	Years	uniform	min = 16 max =200	uninformed
nAge	Power of relative age in fage	-	uniform	min = 0.2 max = 4.0	uninformed
rAge	Relative age to where fage = 0.5	-	uniform	min = 0.01 max = 3.00	uninformed
FR1	Fertility rating parameter 1 (mean annual temperature coefficient)	-	uniform	min = 0.0 max = 1.0	uninformed
FR2	Fertility rating parameter 2 (site index age 25 coefficient)	-	uniform	min = 0.0 max = 1.0	uninformed
Mortality					
wSx1000	Maximum stem mass per tree at 1000 trees/ha	$kg\ tree^{-1}$	normal	mean = 235 sd = 25	2,5,6
ThinPower	Power in self thinning law	-	uniform	min = 1.0 max = 2.5	2,5,6
ms	Fraction of mean stem biomass per tree on dying trees	-	uniform	min = 0.1 max = 1.0	uninformed
Rttover	Average monthly root turnover rate	$month^{-1}$	uniform	min = 0.017 max = 0.042	7

MortRate	Density independent mortality rate (pines)	$month^{-1}$	uniform	min = 0.0002 max = 0.004	uninformed
Understory hardwoods					
alpha_h	Canopy quantum efficiency (understory hardwoods)	mol C mol PAR^{-1}	uniform	min = 0.005 max = 0.07	uninformed
pFS_h	Ratio of foliage to stem partitioning (understory hardwoods)	-	uniform	min = 0.2 max = 3.0	uninformed
pR_h	Ratio of foliage to fine roots (understory hardwoods)	-	uniform	min = 0.05 max = 2	uninformed
SLA_h	Specific leaf area (understory hardwoods)	$m^2\ kg^{-1}$	normal	mean = 16 sd = 3.8	8
fCalpha700_h	Proportional increase in canopy quantum efficiency between 350 and 700 ppm CO_2 (understory hardwood)	-	uniform	min = 1.00 max = 2.5	uninformed

939
940 [1]Albaugh et al., 2005; [2]Gonzalez-Benecke et al., 2016; [3]Gonzalez-Benecke et al., 2014 [4]DeLucia et al., 2007;[5]Bryars et al., 2013;[6]Subedi et al.,
941 201);[7]Matamala et al., 2003; [8]LeBauer et al., 2010; uninformed priors had large, ecologically reasonable bounds.
942

943

Table 4. Description of the different data assimilation approaches used.

Simulation Name	Treatments included in assimilation	Number of plots
Base	All plots and experiments in the region were used simultaneously. Includes unique pCRS, wSx1000, and ThinPower parameters for plots in the Duke FACE study	294
NoExp	Same as Base assimilation but excluding all plots with experimental manipulations. Includes control plots that are part of experimental studies.	208
NoDkPars	Same as Base assimilation but without pCRS, wSx1000, and ThinPower parameter for plots in the Duke FACE and US-DK3 studies	294

944
945

946

Table 5. The optimized medians, range of the 99% quantile intervals of the posterior distributions and the 99% quantile range for priors with normally distributed priors or the range of the upper and lower bounds for priors with uniform distributions.

Parameter	Posterior median	Posterior 99% C.I. range	Prior range	Posterior/Prior Range
Allocation and structure				Parameter group mean = 0.38
pFS2	0.58	0.55 - 0.61	0.08 – 1.00	0.06
pFS20	0.57	0.55 - 0.59	0.10 – 1.00	0.05
pR	0.11	0.07 - 0.15	0.05 – 2.00	0.04
pCRS	0.26	0.25 - 0.27	0.15 - 0.35	0.11
pCRS (Duke)	0.21	0.18 - 0.23	0.15 - 0.35	0.20
SLA0	8.44	7.67 - 9.25	4.4 - 6.66	0.70
SLA1	2.84	2.72 - 2.96	3.59 - 4.16	0.43
tSLA	4.13	3.88 - 4.41	0.43 - 11.51	0.05
fCpFS700	0.74	0.60 - 0.90	0.50 – 1.00	0.60
StemConst	0.022	0.009 - 0.035	0.009 - 0.035	1.00
StemPower	2.78	2.29 - 3.27	2.25 - 3.29	0.95
Canopy photosynthesis, autotrophic respiration, and transpiration				Parameter group mean = 0.14
alpha	0.029	0.026 - 0.031	0.02 - 0.06	0.14
y	0.50	0.47 - 0.53	0.30 - 0.65	0.15
MaxCond	0.011	0.01 - 0.012	0.005 - 0.03	0.09
LAIgcx	2.2	2.0 - 2.48	2.0 - 5 .0	0.16
Environmental modifiers of photosynthesis and transpiration				Parameter group mean = 0.61
kF	0.16	0.12 - 0.2	0.14 - 0.22	1.04
Tmin	-5.56	-8.88 - -2.69	-1.15 - 9.15	0.60
Topt	23.42	21.1 - 26.31	19.85 - 30.15	0.51
Tmax	39.56	34.71 - 44.39	32.85 - 43.15	0.94
SWconst	1.09	0.91 - 1.56	0.01 - 1.8	0.36
SWpower	8.86	3.39 - 12.98	1.00 – 13.00	0.80
CoeffCond	0.036	0.029 - 0.043	0.034 - 0.048	0.91
fCalpha700	1.33	1.18 - 1.52	1.0 - 1.80	0.43
MaxAge	151.5	54.4 - 199.6	16.0 - 200 .0	0.79
nAge	3.35	1.77 - 3.99	1.00 – 4.00	0.74
rAge	2.25	0.81 - 2.99	0.01 – 3.00	0.73
FR1	0.073	0.061 - 0.086	0.00 – 1.00	0.03
FR2	0.17	0.15 - 0.19	0.0 – 1.0	0.04
Mortality				Parameter group mean = 0.37
wSx1000	176.9	169.6 - 184.4	165.6 - 294.4	0.15
wSx1000 (Duke)	243.3	196.89 - 305.02	165.6 - 294.4	0.76

ThinPower	1.68	1.60 - 1.78	1.00 - 2.5	0.12
ThinPowerv(Duke)	1.26	1.00 - 1.85	1.00 - 2.5	0.56
mS	0.52	0.37 - 0.71	0.10 – 1.00	0.38
Rttover	0.023	0.017 - 0.031	0.017 - 0.042	0.55
MortRate	0.001	9e-04 - 0.0011	2e-04 - 0.004	0.06
Understory hardwoods				Parameter group mean = 0.28
alpha_h	0.02	0.02 - 0.02	0.005 - 0.07	0.01
pFS_h	1.78	1.54 - 2.06	0.2 – 3.0	0.19
pR_h	0.21	0.06 - 0.43	0.05 – 2.00	0.19
SLA_h	16.3	14.1 – 19.0	6.2 - 25.8	0.25
fCalpha700_h	1.84	1.58 - 2.17	1.0 – 2.50	0.74

Table 6. Median and range of the 99% quantile intervals of the posterior distributions for the parameters in the NoExp and NoDkPars assimilations

Parameter	NoExp median	NoExp 99% range	NoDkPars median	NoDkPar 99%
Allocation and structure				
pFS2	0.63	0.61 - 0.68	0.57	0.55 - 0.60
pFS20	0.63	0.60 - 0.65	0.57	0.55 - 0.59
pR	0.11	0.06 - 0.16	0.11	0.08 - 0.15
pCRS	0.29	0.27 - 0.30	0.26	0.25 - 0.27
pCRS (Duke)	0.25	0.23 - 0.28	N/A	N/A
SLA0	7.47	6.57 - 8.41	8.56	7.73 - 9.32
SLA1	3.00	2.88 - 3.12	2.89	2.79 - 2.99
tSLA	4.75	4.30 - 5.26	4.12	3.90 - 4.38
fCpFS700	0.50	0.50 - 0.53	0.94	0.83 – 1.00
StemConst	0.022	0.01 - 0.04	0.02	0.01 - 0.04
StemPower	2.79	2.27 - 3.26	2.77	2.28 - 3.30
Canopy photosynthesis, autotrophic respiration, and transpiration				
alpha	0.030	0.028 - 0.033	0.029	0.026 - 0.031
y	0.48	0.45 - 0.51	0.49	0.46 - 0.52
MaxCond	0.017	0.015 - 0.021	0.011	0.011 - 0.012
LAIgcx	4.4	3.9 – 5.0	2.1	2.0 - 2.5
Environmental modifiers of photosynthesis and transpiration				
kF	0.15	0.11 - 0.20	0.16	0.11 - 0.20
Tmin	-7.8	-10.97 - -4.95	-6.04	-9.06 - -3.03
Topt	21.55	19.15 - 24.39	22.71	20.54 - 25.42
Tmax	40.56	36.51 - 45.62	39.82	35.62 - 44.56
SWconst	0.93	0.8 - 1.1	1.14	0.91 - 1.62
SWpower	6.27	2.98 - 11.49	7.99	3.29 - 12.95
CoeffCond	0.041	0.034 - 0.047	0.036	0.030 - 0.042
fCalpha700	1.01	1.0 0- 1.06	1.15	1.10 - 1.25
MaxAge	152.84	54.18 - 199.5	152.0	49.2 - 199.3
nAge	3.36	1.93 - 3.99	3.36	1.89 - 3.99
rAge	2.26	0.80 - 2.99	2.24	0.83 - 2.99
FR1	0.12	0.09 - 0.14	0.08	0.07 - 0.09
FR2	0.20	0.16 - 0.24	0.17	0.15 - 0.19
Mortality				
wSx1000	191.6	180.2 - 210.2	181.32	173.26 - 196.32
wSx1000 (Duke)	235.1	175.0 - 297.5	N/A	N/A
ThinPower	1.76	1.61 - 1.92	1.59	1.46 - 1.72
ThinPower (Duke)	1.42	1.01 - 2.02	N/A	N/A

mS	0.54	0.33 - 0.80	0.5	0.25 - 0.71
Rttover	0.019	0.02 - 0.03	0.022	0.017 - 0.030
MortRate	0.0013	0.0011 - 0.0014	0.0011	9e-04 - 0.0013
Understory hardwoods				
alpha _h	0.031	0.025 - 0.040	0.02	0.017 - 0.023
pFS_h	2.39	1.86 - 2.96	1.79	1.59 - 2.09
pR_h	0.25	0.05 - 0.67	0.21	0.06 - 0.41
SLA_h	12.37	9.96 - 15.07	16.42	14.37 - 18.55
fCalpha700_h	1.08	1.00 - 1.83	1.83	1.56 - 2.15

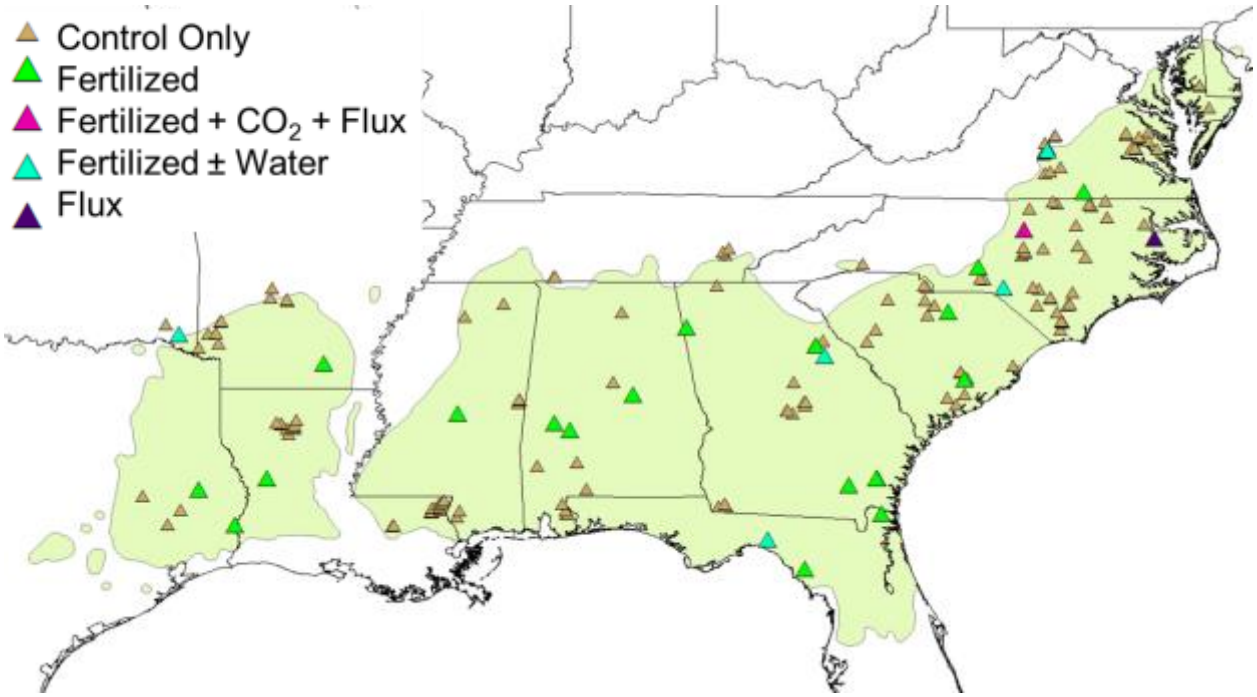

Figure 1. Map of loblolly pine distribution, plot locations used in data assimilation, and the experiment type associated with each plot. The control-only treatments were plots without any associated experimental treatment or flux measurements. Fertilized were plots with nutrient additions. CO_2 were plots with free-air concentration enrichment treatments. The flux treatments were plots with eddy-covariance measurements of ecosystem-scale carbon and water exchange. The water treatments included throughfall exclusion and irrigation experiments.

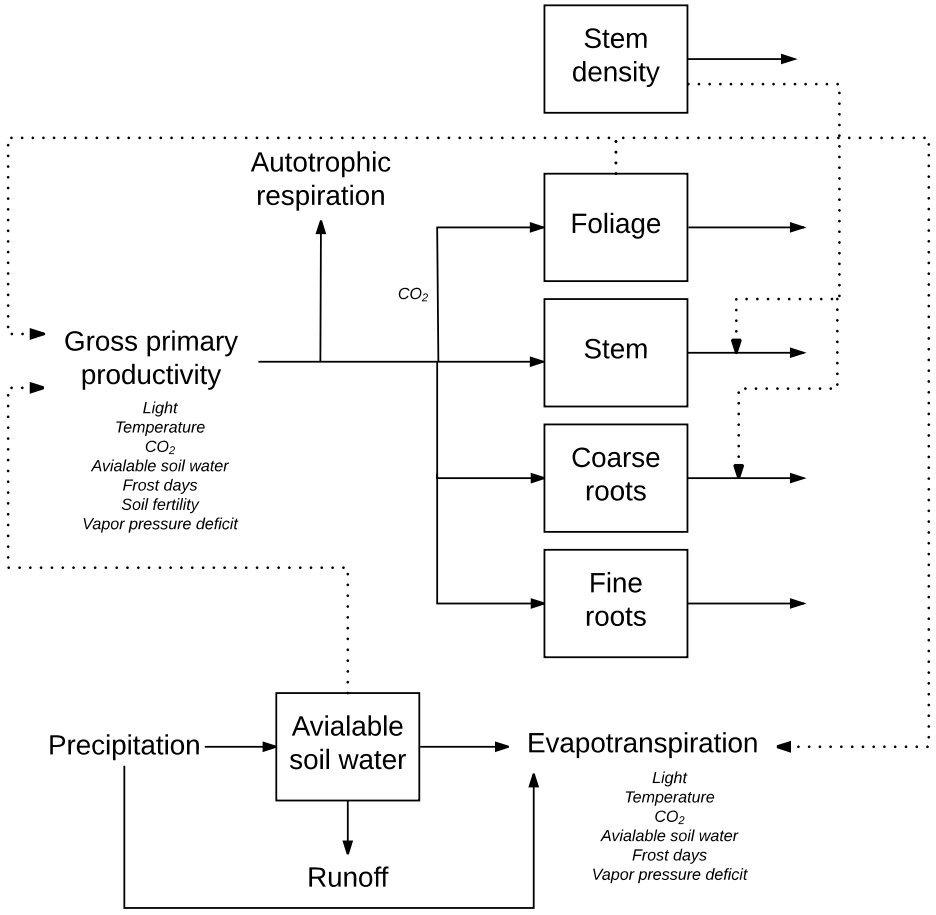

Figure 2. A diagram of the monthly time-step 3-PG model used in this study. The stocks are represented by the boxes and the fluxes by the arrows. An influence of a stock on a flux that is not directly related to that stock is represented by the dotted lines. The environmental influences on a flux is described using italics. A description of the model can be found in the supplemental information.

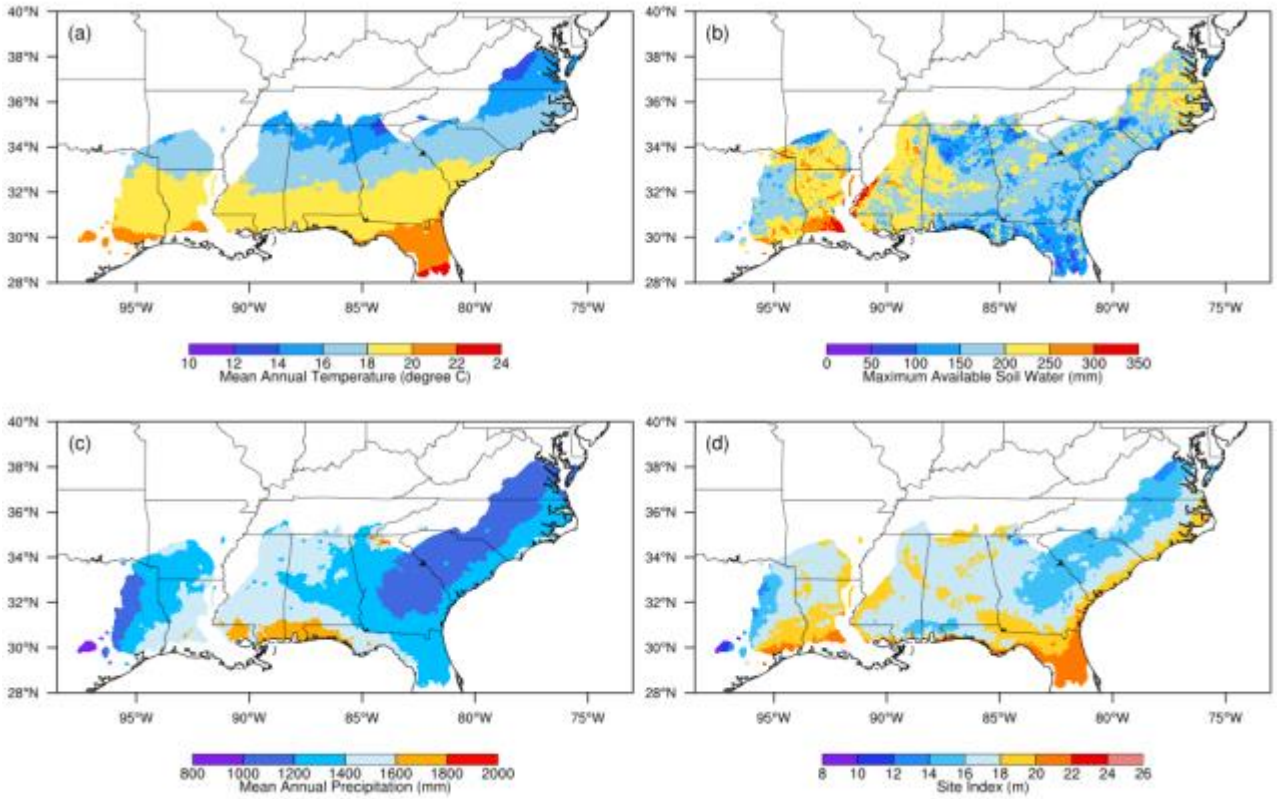

Figure 3. Key climatic and stand characteristic inputs to the regional 3-PG simulations: (a) Mean annual temperature (1979-2011) as a summary of the gradient in monthly temperature inputs used in simulations, (b) maximum available soil water for the top 1.5 meters of soil from SSURGO, (c) mean annual precipitation (1979-2011) as a summary of the gradient in monthly precipitation inputs used in simulations, and (d) site index. The area shown is the natural range of loblolly pine (*Pinus taeda L.*).

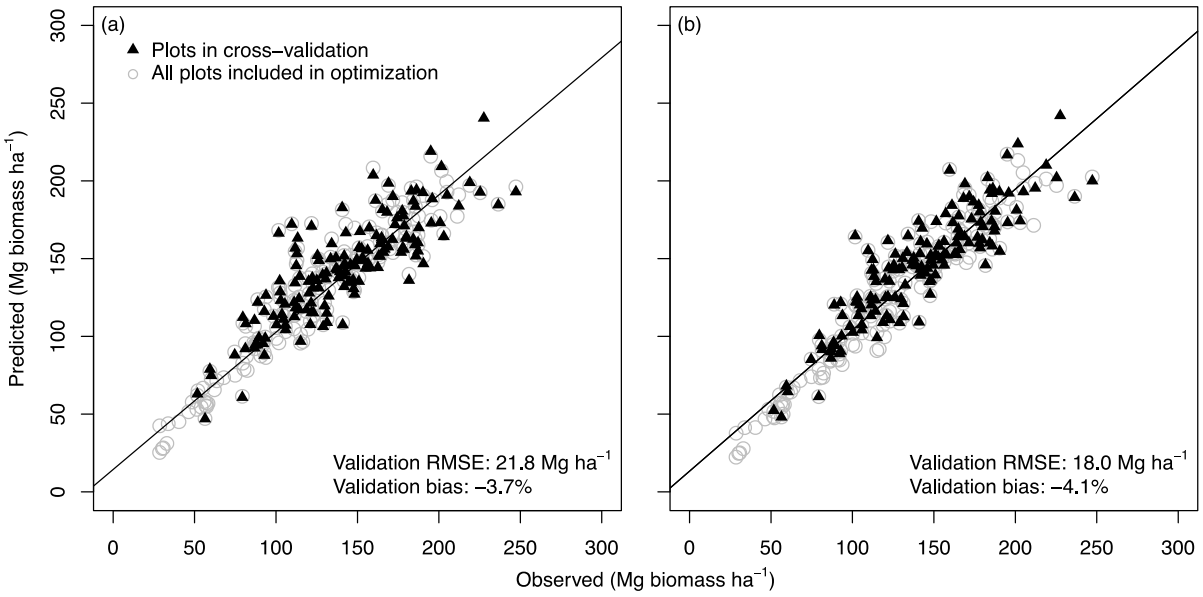

Figure 4. Model evaluation of stem biomass when assimilating (a) observations across environmental gradients and ecosystem manipulation experiments (Base; Table 4), and (b) assimilation only observations across environmental gradients (NoExp; Table 4). The gray circles correspond to predictions where all plots were used in data assimilation. The black triangles correspond to predictions where 160 plots were not included in data assimilation and represent an independent evaluation of model predictions (out-of-bag validation). For each plot, we used the measurement with the longest interval between initialization and measurement for evaluation.

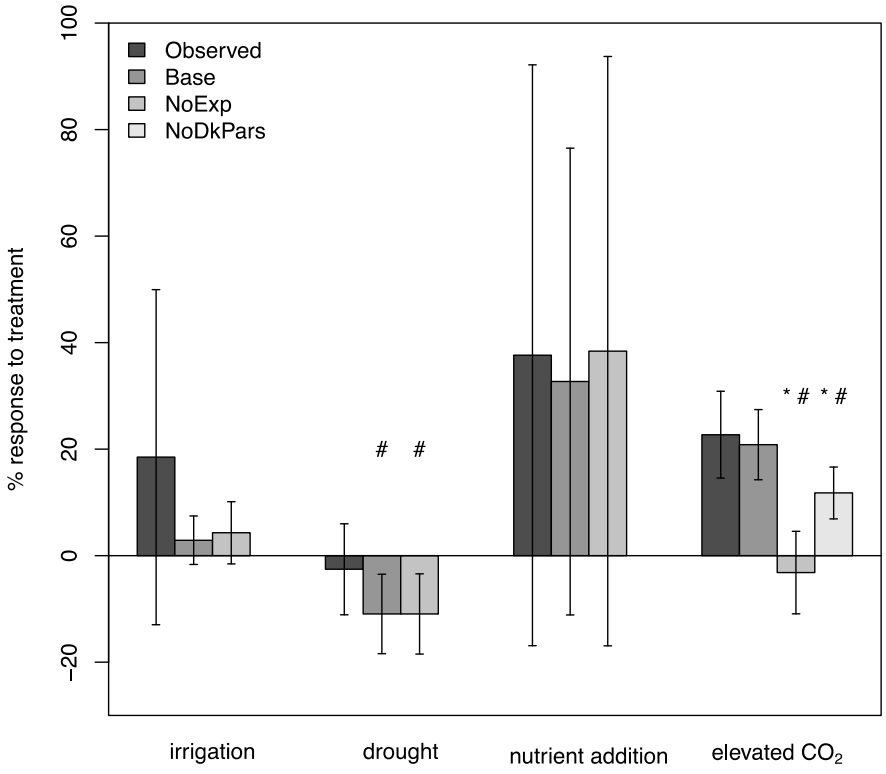

Figure 5. The mean response, expressed as a percentage change in stem biomass from the control treatment, for irrigation, drought (as a reduction in throughfall), nutrient addition, and elevated CO_2 experiments. The observed response and the response simulated by the Base, NoExp, and NoDkPars assimilation approaches are shown. # signifies that value below marker was significantly different from the observed response ($p < 0.05$). * signifies that value below marker was significantly different from the response in the Base assimilation ($p<0.05$). Error bars are ±1 standard deviation.

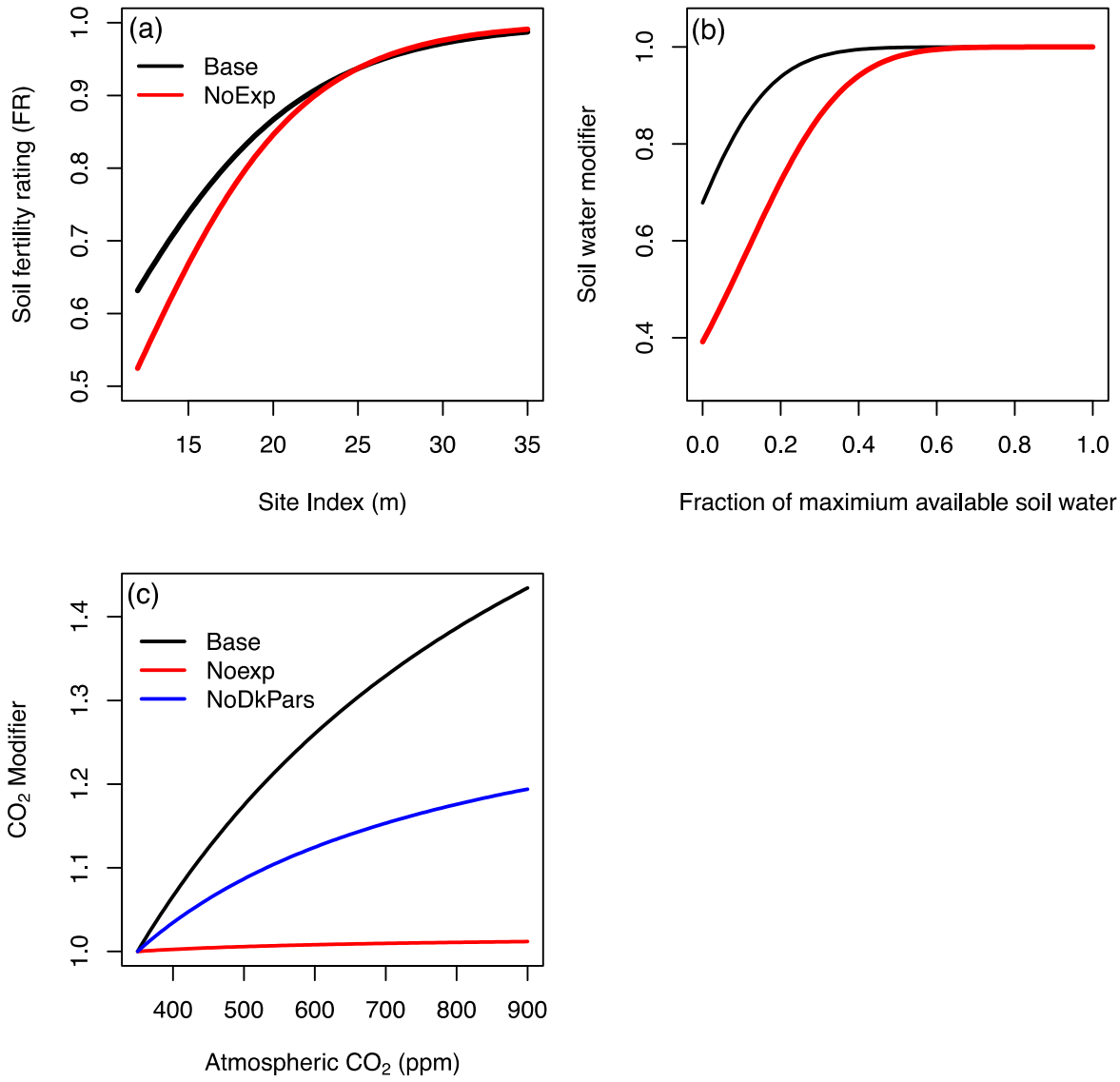

Figure 6. Optimized environmental response functions in the 3-PG model for the (a) soil fertility influence on photosynthesis), (b) available soil water influence on photosynthesis and conductance, and (c) atmospheric CO_2 influence on photosynthesis. The function shapes were derived from the parameters in the Base, NoExp, and NoDkPars assimilations (Table 4).

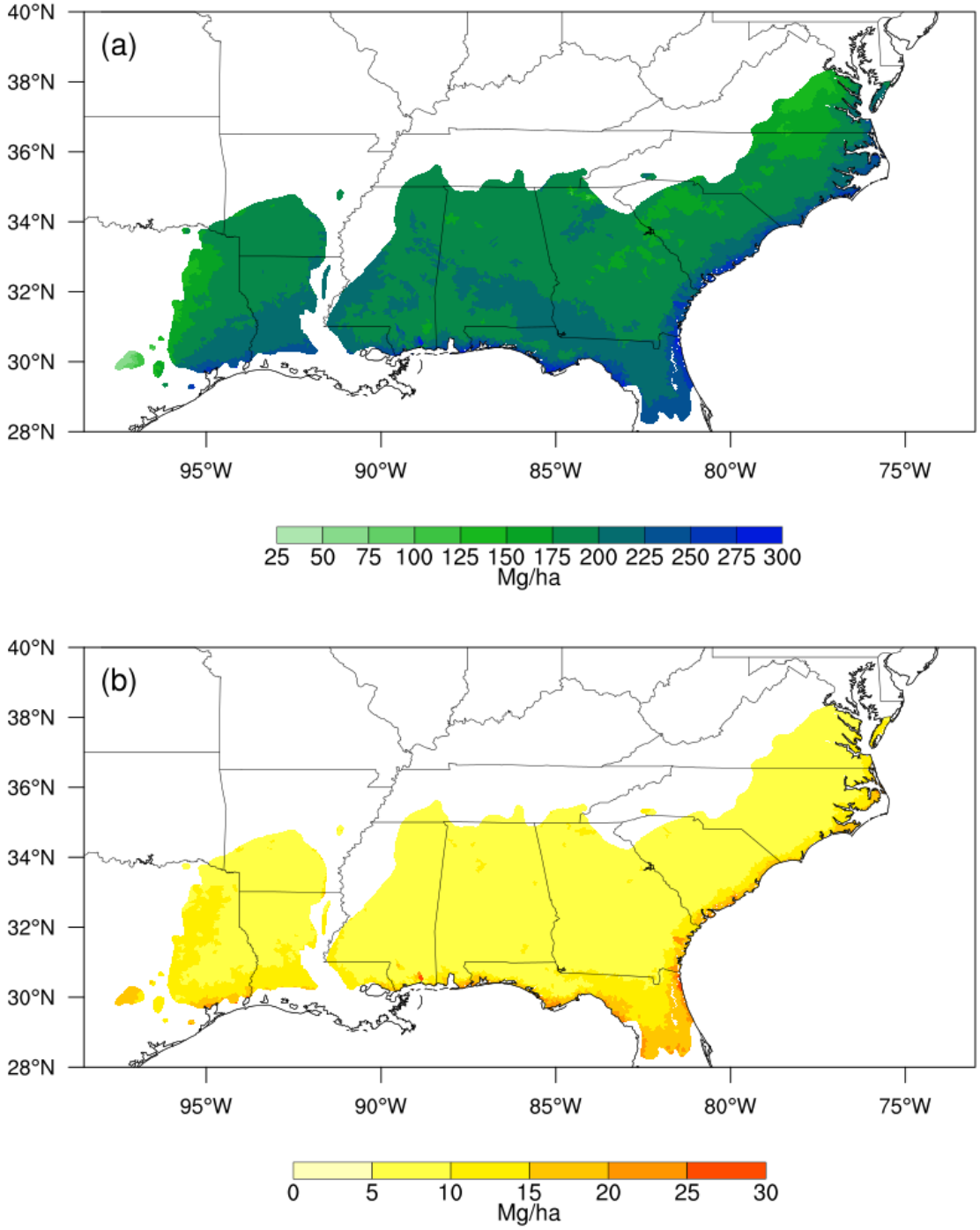

Figure 7. (a) Regional predictions of stem biomass stocks for a 25-year-old stand planted in 1985. Parameters used in the predictions were from the Base assimilation approach described in Table 5. (b) The width of the 95% quantile interval associated with uncertainty in model parameters.

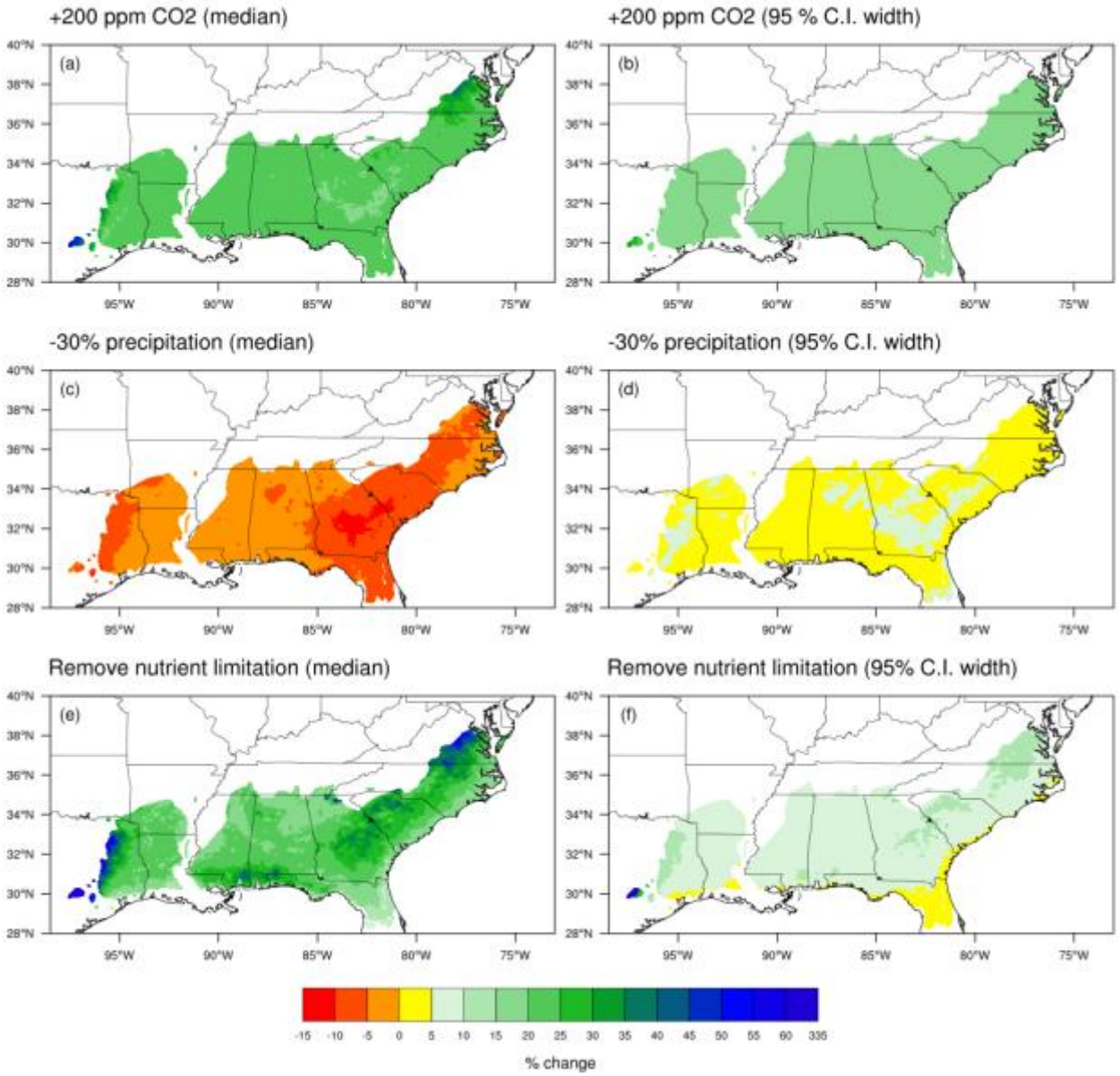

Figure 8. Predictions of the percentage change in stem biomass at age 25 in response to (a,b) a 200 ppm increase in atmospheric CO_2 over 1985-2011 concentrations, (c,d) a 30% reduction in precipitation from 1985-2011 levels, and (e,f) a removal of nutrient limitation by setting the soil fertility rating in the model equal to 1. The left column is the median prediction and the right column is the width of the 95% quantile interval associated with parameter uncertainty. The predictions used the Base assimilation.